

Aus der Orthopädischen Klinik und Poliklinik der
Ludwig-Maximilians-Universität München

Direktor: Prof. Dr. med. Dipl.-Ing. V. Jansson

**Chondrogenic differentiation and proliferation potential of human
adipose-derived stem cells combined porous chitosan-based
scaffolds for articular cartilage formation *in vitro***

Dissertation

zum Erwerb des Doktorgrades der Humanbiologie
an der Medizinischen Fakultät der
Ludwig-Maximilians-Universität zu München

vorgelegt von

Yijiang Huang
aus
Zhejiang, China

Jahr

2019

**Mit Genehmigung der Medizinischen Fakultät
der Universität München**

Berichterstatter: Prof. Dr. med. Peter E. Müller

Mitberichterstatter: Priv. Doz. Dr. med. Thomas Niethammer
Priv. Doz. Dr. med. Stefan Grote

Mitbetreuung durch den
promovierten Mitarbeiter: Dr. Roland M. Klar

Dekan: Prof. Dr. med. dent. Reinhard Hickel

Tag der mündlichen Prüfung: 13.03.2019

To my family

Eidesstattliche Versicherung

Huang Yijiang

Name, Vorname

Ich erkläre hiermit an Eides statt,
dass ich die vorliegende Dissertation mit dem Thema

Chondrogenic differentiation and proliferation potential of human adipose-derived stem cells combined porous chitosan scaffold for articular cartilage formation *in vitro*

selbständig verfasst, mich außer der angegebenen keiner weiteren Hilfsmittel bedient und alle Erkenntnisse, die aus dem Schrifttum ganz oder annähernd übernommen sind, als solche kenntlich gemacht und nach ihrer Herkunft unter Bezeichnung der Fundstelle einzeln nachgewiesen habe.

Ich erkläre des Weiteren, dass die hier vorgelegte Dissertation nicht in gleicher oder in ähnlicher Form bei einer anderen Stelle zur Erlangung eines akademischen Grades eingereicht wurde.

Munich, 13.03.2019

Ort, Datum

Yijiang Huang

Unterschrift Doktorandin/Doktorand

Table of Contents

1	Introduction.....	4
1.1	Chondrogenesis.....	4
1.2	Pathologies of articular cartilage.....	9
1.3	Articular cartilage treatments.....	11
1.3.1	Routine clinical articular cartilage treatments.....	13
1.3.2	Regenerative articular cartilage repair.....	17
1.4	Stem cells in articular cartilage repair.....	18
1.5	Biomaterials and cartilage repair.....	21
2	Hypothesis of the Study.....	23
3	Aims and Objectives	23
4	Materials and methods.....	24
4.1	1% Porous chitosan constructs (PCS)	24
4.2	Isolation and culture of human Adipose-Derived Stem Cells.....	25
4.3	Cell seeding onto PSCs and <i>in vitro</i> chondrogenic differentiation.....	26
4.4	Pellet culture and chondrogenic differentiation.....	27
4.5	Scanning electron microscopy (SEM).....	27
4.6	Cell Viability and Proliferation assay.....	28
4.7	Cell survival in the scaffold.....	28
4.8	Histological analysis and Immunofluorescence staining.....	29
4.9	Quantitative real-time PCR (qRT-PCR) analysis of chondrogenic differentiation....	30
4.9.1	Gene primer design and optimisation.....	31
4.9.2	cDNA standardization for qRT-PCR.....	32
4.9.3	Stability and quantity of reference primers (GeNorm)	33
4.9.4	qRT-PCR.....	34
4.10	Statistics.....	35
5	Results.....	36
5.1	Characterization of the porous chitosan scaffold and seeding with differentiated ADSCs	3

5.2 Viability and proliferation of hADSCs on chitosan scaffolds.....	38
5.3 Cell survival with Live/Dead Assay in porous chitosan scaffolds.....	39
5.4 Histology analyses of chitosan scaffold culture.....	41
5.5 Pellet Culture results and histology analyses.....	43
5.6 Immunofluorescence analyses.....	47
5.7 QRT-PCR results.....	52
5.7.1 Optimum Amplification Temperature of all gene primers.....	52
5.7.2 Standardized cDNA quantity for optimum qRT- PCR reactions.....	53
5.7.3 GeNorm: Stability and optimal number of reference gene(s).....	54
5.7.4 qRT-PCR of <i>in vitro</i> chondrogenic differentiation.....	56
6 Discussion.....	62
7 Conclusion.....	70
8 Summary.....	71
9 Zusammenfassung.....	73
10 References.....	75
11 List of figures and tables.....	103
12 Abbreviations.....	104
13 Acknowledgment.....	106

1. Introduction

Regenerating articular cartilage degeneration due to age or extreme sports-related excursions remains one of the major challenges of tissue regenerative sciences (Hunter 1743). For nearly three centuries since a re-visitation by Hunter on the many observations of Hippocrates on the healing aspect of various tissue types and organs, the problem at successfully healing the cartilage of joints by filling the defect parts with a tissue that has the same mechanical properties as hyaline cartilage and effectively integrates at the defect site without becoming ossified with time (Campbell 1969; Caplan, et al. 1997; Fuller and Ghadially 1972; Ghadially, et al. 1977; Hunter 1743; Kim, et al. 1991; Mankin 1982; Silver and Glasgold 1995), remains a problem still faced in the 21st century (Hangody, et al. 2001). The introduction with associated literature review brings to light the many aspects of this unique enigma providing new prospects that to date are not properly considered or have been ignored in light of a burgeoning pharmaceutical sector intent on providing quick fixes instead of long-term solutions.

1.1 Chondrogenesis

Chondrogenesis is a specialized process that occurs as a result of mesenchymal cell condensation and chondroprogenitor cell differentiation (Goldring, et al. 2006). Following chondrogenesis, the chondrocytes remain in a quiescent phase from which then either the cartilage anlage develops that will then form parts of the bones of the skeleton, in the process of endochondral osteogenesis, or develop the highly specialized connective tissue that covers the weight-bearing surfaces of diarthrodial joints, whose principal functions are to provide a smooth, lubricated surface for the joint and to facilitate the

transfer of a load with a low coefficient of friction termed articular cartilage (Sophia Fox, et al. 2009).

- **Endochondral bone formation**

The endochondral bone formation is the process during the 8th week of fetal development in the mammalian skeleton system, involving mesenchymal progenitor cells differentiating into chondrocytes which are responsible for depositing a cartilaginous framework that is later mineralized and replaced by bone tissue (de Crombrughe, et al. 2001). Endochondral osteogenesis is an essential process occurring in the development and growth of long bones including the method by which fractures are healed within these bone types (Brighton and Hunt 1986; Scammell and Roach 1996).

There are five stages to endochondral ossification as follows: (1) Mesenchymal stem cells (MSCs) condensate and proliferate; (2) MSCs differentiate into chondrocytes; (3) chondrocytes synthesize cartilage extracellular matrix (ECM); (4) hypertrophy occurs and matrix mineralization (5) endochondral ossification.

Before the first phase of endochondral ossification, during embryogenesis, begins, the spatiotemporal pattern causes mesenchymal stem cells to migrate and localize to the region where bones will develop (Kovacs 2011). The first stage of endochondral ossification is achieved by the interaction of fibroblast growth factor (FGF) expression and the Hedgehog pathway signals (Quintana, et al. 2009), where mesenchymal cells

aggregate, condense and undergo hyper-proliferation to form a skeletal bone cellular model (Alborzi, et al. 1996; Kovacs 2011; Quintana, et al. 2009). Proliferated mesenchymal cells then differentiate into chondrocytes, the cartilage cells, and begin to secrete a cartilage-specific extracellular matrix skeleton form, in which bone formation will occur (Gilbert 2000; Quintana, et al. 2009). In the fourth stage of the endochondral ossification process, chondrocytes stop proliferating and increase their size dramatically, becoming hypertrophic chondrocytes that alter the matrix and produce collagen type X and fibronectin which subsequently are mineralized by calcium phosphates or as is more commonly termed hydroxyapatite (Gilbert 2000; Kovacs 2011). The transcription factor *sex determining region Y-box 9 (SOX9)* is expressed during the early stages to regulate the differentiation of the chondrocyte, whereas *runt-related transcription factor 2 (RUNX2)* expression is initiated during the hypertrophic differentiation (Hattori, et al. 2010). Also, other regulating factors such as bone morphogenetic proteins (*BMPs*) and *wingless-type MMTV integration site family (Wnts)* signals are involved in these processes (Day and Yang 2008; Mackie, et al. 2008). However, a small portion of chondrocytes is converted into chondroclasts and specialized cells, which are critical for the final stages of the endochondral osteogenic process (Kovacs 2011). This is followed by the invasion of osteoblast progenitors, osteoclasts, hematopoietic cells and blood vessel endothelial cells from the perichondrium into the hypertrophic cartilage. The chondroclasts dissolve the hypertrophic cartilage through lysosomal enzymes, the incoming osteoprogenitor stem cells differentiate into trabecular bone-forming osteoblasts, together with hematopoietic and endothelial cells to establish bone marrow in which becomes the primary ossification centre (Gilbert 2000; Maes, et al. 2010). The osteoblasts then deposit osteoid matrix on the partially degraded cartilage as a template,

mainly including osteocalcin, chondroitin and collagen type I (Gilbert 2000; Hatori, et al. 1995). Eventually, the osteoid is replaced by new bone through mineralization including the penetration by mineral salts, in particular, calcium and phosphate ions to the matrix (Bruder and Caplan 1989). After these processes, two ossification centres are then formed: the cartilage template is first invaded at its centre and later at each end by a mixture of cells that establish the primary and secondary centres of ossification. These centres subsequently and gradually invade the remaining cartilage, ultimately replacing it with bone thereby reaching skeletal maturity, except for the articular surface occupied by articular cartilage (Mackie, et al. 2008).

- **Articular chondrogenesis**

Three different cell germ layers are formed during embryogenesis, called mesoderm, ectoderm and endoderm. After four weeks of gestation, mesenchymal stem cells (MSCs), derived from the mesoderm, grow into the components of the appendicular skeleton (Hall and Miyake 1992). MSCs experience cell-substrate and cell-cell interactions over the development of the limbs, resulting in cell aggregation and advanced mitosis, thus increasing cell density within the condensate (Vogel and Sheetz 2006). Before the condensation, the pre-chondrocyte MSCs produce ECM rich in hyaluronic acid and collagen type I. During the condensation the cells synthesize hyaluronidase and cell adhesion molecules, leading to a decreased concentration of hyaluronic acid and thus a closer cell-cell contact. Transforming growth factor-beta (TGF- β) signalling induces the expression of the *SOX9*, which is required for *collagen type II (Col2)* and *aggrecan (ACAN)* expressing during early condensation (de

Crombrugge, et al. 2000). At the end of the condensation process, the expression of the intracellular signalling pathway activates, thereby initiating the transformation of the chondrocyte progenitor cells into mature chondrocytes(DeLise, et al. 2000). After the gestation from 4 to 7 weeks, these prechondrogenic MSCs undergo condensation that gives rise to cell aggregates, which then continue to differentiate into two distinct chondrogenic lineages: persistent chondrocytes and proliferating chondrocytes, which excrete large amounts of collagen and ECM for forming hyaline cartilage, and form the growth plate, respectively (Pacifici, et al. 2006).

Chondrogenesis differentiation is an intricate process that results in a cartilage intermediate, leading to articular cartilage formation and endochondral ossification during development. The proliferating chondrocytes eventually become hypertrophic, which produce individual growth factors that promote blood vessels extension. After initial chondrocyte angiogenesis and osteoblasts, derived from MSCs, these secrete a matrix material that leads to mineralization and formation of the bone collar, where the first ossification centre occurs (Thompson, et al. 1989) and continues to grow into the trabecular bone which promotes continued bone elongation. A second ossification centre then forms at the other end of the cartilage anlage, thereby enclosing the hyaline cartilage in the interzone (Kronenberg 2003), followed by cavitation and finally formation of joint structures. However, the prechondrogenic cells originating from the interzone continue to condensate, differentiate into persistent chondrocytes which produce matrix components such as collagen type II and aggrecan, with collagen type I production turned off, resulting in the development of the articular cartilage. The matured

chondrocytes are then entrapped in their ECM and obtain a characteristic round phenotype (Holtzer 1964).

The cellular processes involved in articular cartilage formation reveal essential insights and guide regenerative science towards developing improved therapies. The cell activity and phenotypic state, as well as production and structural composition of the ECM, change significantly through the condensation, differentiation of prechondrogenic mesenchymal cells during the embryonic stages until maturation and also in the processes of the articular cartilage formation from limb buds (Jadin, et al. 2005). At the early stage, chondrocytes proliferate and produce components of the ECM resulting in tissues with dense cells. As a response to the corresponding applied mechanical forces, the articular cartilage is remodelled by changing its composition and structure in the maturity phase, leading to an increase of the birefringence of the tissue (Armstrong and Gardner 1977; Hunziker, et al. 1997). Articular cartilage reaches maturation consistently with the maturity of the skeleton, when chondrocytes almost stop proliferating and excreting ECM, living in a quiet and stable stage (Jadin, et al. 2005).

1.2 Pathologies of articular cartilage

Articular cartilage remains, due to its avascular structure and limited nerve regulation, a tissue, unlike bone, that has extreme difficulties at regenerating or healing itself, even when minimally damaged (Chiang and Jiang 2009; Loeser, et al. 2012; Wang, et al. 2006; Wang, et al. 2014). Damage from injury or degenerative pathologies frequently results in gradual tissue deterioration, leading to debilitating joint effusion, joint pain,

functional impairment and degenerative arthritis(Centers for Disease and Prevention 1994; Lawrence, et al. 1998). There are generally two groups of articular cartilage lesions: partial-thickness (chondral) and full-thickness (osteochondral) defects.

A chondral defect, referring to a focal area of damage to the articular cartilage, can be the result of direct blunt trauma, accidental and sudden joint loading, and torsional injuries (Buckwalter 1998; Campbell 1969; Newman 1998). It leads to a brief metabolic and enzymatic response, which produces enough new chondrocytes to repair superficial defects spontaneously (Fuller and Ghadially 1972; Ghadially, et al. 1977; Hunziker and Rosenberg 1996; Kim, et al. 1991). In osteochondral defect in which the defect penetrates the subchondral bone resulting in an intense inflammatory response together with the release of cytokines and growth factors, such as interleukin-1 (IL-1), the matrix metalloproteinases (MMP) and TGF- β supergene family protein members, jointly promote tissue lysis and mesenchymal progenitor stem cell accumulation within the defect site (Caplan, et al. 1997; Ivkovic, et al. 2010; Silver and Glasgold 1995). The progenitor stem cells within the defect site often then differentiate into hypertrophic chondrocytes which together with the invasion of new blood vessels and new bone marrow formation penetrate the defect site eventually leading to the formation of fibrocartilage instead of the required articular cartilage matrix reformation, which is inferior to hyaline cartilage in structure and mechanical competence(Campbell 1969; Caplan, et al. 1997; Shapiro, et al. 1993).

The incidence and prevalence of partial thickness chondral defects within joints are difficult to detect as many lesions within the articular surface are “silent” or undetectable

where it is clear that it is precisely these asymptomatic defects that are the ones that advance and progress from partial-thickness chondral lesions to the more full-thickness severe osteochondral defects. Curl et al. (1997) analysis from 31000 knee arthroscopic procedures discovered that 63% of the chosen sample size of patients with asymptomatic knees had chondral lesions (Curl, et al. 1997). This was also supported by Widuchowski et al. (2007) after evaluating over 25,000 knee arthroscopy samples, it was found that 60% of patients had chondral lesions and 58% patients' symptoms of articular cartilage lesions which were as a direct result from traumatic, noncontact mechanism of injury (Widuchowski, et al. 2007). On the other hand, degenerative chondral changes mainly occur in elderly patients due to arthritic changes, which make the cartilage in a joint to become soft and lose its elasticity, making it more sensitive to injuries and leading to a large area of focal lesions.

Other pathologies, meniscal injuries or deficiency, malalignment, and ligamentous instability that are known to contribute to the development of articular cartilage lesions, are frequently encountered by the operating surgeon treating articular cartilage defects (Breinan, et al. 1997; Joshy, et al. 2010; Mandelbaum 2016; Shelbourne, et al. 2003). It has been demonstrated that chondral injuries may accompany an injury to a ligament such as the anterior cruciate ligament (ACL) and meniscus (Tandogan, et al. 2004). The ligament tear of the knee joint may cause and accelerate the cartilage defect, which may need to be reconstructed before or at the same time to re-lay the cartilage surface to slow the development of arthritis (Engebretsen, et al. 1988). Furthermore, patients with cartilage lesions due to lack of meniscus are likely to have no successful cartilage surface replacement unless replaced by a new meniscus. In these cases, it may be

beneficial to conduct an appropriate assessment and examination of potential meniscal transplants(Lohmander, et al. 2007).

1.3 Articular cartilage defect treatments

There are two fundamental problems which need to be addressed in the repair of articular cartilage which are that : (1) the tissue utilized to restore an articular cartilage defect site has the same mechanical properties as hyaline cartilage, whilst (2) effectively integrating itself within a defect site without undergoing endochondral bone formation (Rubak, et al. 1982). Even a small defect caused by mechanical damage tends to degenerate progressively over time towards osteoarthritis. Clinically, orthopaedic surgeons treat chondral lesions depending on patient selection, daily sports activities, age, grade and quality of the cartilage defect. The options of treatment range from conservative, through outdated and ineffective conventional arthroscopic surgical techniques of repair, mainly including abrasion arthroplasty, chondrectomy, micro-fracture of the subchondral bone, perichondria or periosteal resurfacing and the transplantation of autologous or allogeneic osteochondral grafts (Angermann, et al. 2002; Argun, et al. 1993; Breinan, et al. 1997; Chen, et al. 2011; Homminga, et al. 1990). The common target of all utilized methods is to produce a sufficiently stable quality of the cartilage reparation or regeneration, eventually, achieve the restoration of a functioning joint.

1.3.1 Routine clinical articular cartilage treatments

Conservative treatment is considered in the mild symptomatic cases with small chondral defects to relieve the symptoms other than repair cartilage lesion, taking into account

the disadvantages of surgery may harm the right part of the articular (Yasuda 1997). Messner and Maleitus (1996) reported that although about 80% of patients with isolated chondral lesions had good or excellent results undergoing the conservative treatment after a long-term follow-up, most of the patients had abnormal radiographic findings 14 years later. The study revealed that asymptomatic lesions might deteriorate to permanent knee damage (Messner and Maletius 1996).

Current surgical strategies of treatment for articular cartilage defects can be grouped into palliative, reparative, and restorative techniques. Patients with low physical demands and small lesions are firstly considered to have palliative procedures such as arthroscopic lavage and debridement (Dervin, et al. 2003; Harwin 1999), while young patients with high physical demand are considered for a reparative or a restorative treatment. Although the debridement has not been shown to enhance the repair of cartilage lesions, it could alleviate the symptoms such as pain and joint dysfunction. Lavage procedure is the essential irrigation of the inflammatory mediators out from the knee joint. Debridement performed by the simple shaving of fibrotic cartilage surfaces, removing lesion tissue, debris and any loose piece of cartilage from the joint (Sprague 1981). Arthroscopic lavage removes inflammatory mediators, loose cartilage and collagen debris, which can slip into the synovium and cause synovitis and fluid accumulation (Gibson, et al. 1992). Both of these two techniques have been proven to be the best frontline treatment of chondral lesions in the treatment of early stages of osteoarthritis (OA) since the early 1980s (Edelson, et al. 1995; Livesley, et al. 1991; Ogilvie-Harris and Fitsialos 1991).

The most studied reparative technique is micro-fracture, which is a controlled perforation of the subchondral bone plate to permit the pluripotent bone marrow stem cells and growth factors into the site of a cartilage defect which leads to the formation of fibrocartilage (Bae, et al. 2006). The arthroscopic micro-fracture technique uses angled awls to avoid the potential risk of the thermal necrosis, which is more natural and effective than drilling (Hunt, et al. 2002). This reparative fibrocartilage contains a high concentration of type I collagen, which is biochemically and biomechanically inferior to the hyaline articular cartilage that has the properties as type II collagen to resist compression and shear load, appears to deteriorate over time (Kreuz, et al. 2006; Redler, et al. 2012). According to the literature, although about 80% of patients have been relieved of pain and dysfunction in the short term, these results are further deteriorated after about four years (Hunt, et al. 2002; Shannon, et al. 2001).

Those as mentioned above conventional surgical techniques of articular cartilage repair are partially successful in alleviating pain symptoms, but fail to regenerate tissue with the similar properties in nature as native articular cartilage and prompted the development of other new techniques. The restorative techniques, autologous chondrocyte implantation (ACI) (Brittberg, et al. 1994) and autologous osteochondral transplantation (AOT) (Hangody, et al. 2001), aimed to replace damaged cartilage with the formation of fresh hyaline-like cartilage with higher postoperative expectation and are indicated for large symptomatic lesions or prior failed treatment, in high demand patients. ACI is a two-stage procedure. The first stage contains an arthroscopic evaluation of the chondral lesion and performing the biopsy of the healthy hyaline cartilage from a non-weight bearing region of the articular cartilage. The chondrocytes

are released from the ECM by enzymatic digestion and culture expanded *in vitro*. Subsequently, the expanded chondrocytes are harvested and transplanted with fibrin beneath a periosteal flap sutured over the cartilage defect (Grande and Pitman 1988). This surgical technique is widely used in many clinical studies since the last two decades and has shown satisfactory outcomes (Matsusue, et al. 1993; Micheli, et al. 2001; Ohlendorf, et al. 1996).

AOT, on the other hand, involves removal of osteochondral plugs from relatively non-weight bearing areas of the articular cartilage, such as femoral trochlear groove and tibia, and transplant them into debrided defect sites (Campbell, et al. 1963). The advantage of this technique is that osteochondral grafts provide a formed articular cartilage matrix with viable chondrocytes for rapid healing adjacent recurrent tissue and offers an excellent vertical fixation of the osteochondral plug to the implant site through a small incision performed in one procedure. Although it could be used to fill relatively large defects, the application of this technique is limited due to the amount of donor tissue available in the joint (Yamashita, et al. 1985). Some clinical follow-up studies revealed that transplantation of autologous grafts could restore articular surface in patients with large defects and provide proper function of the joint for a longer time (Jacobs 1965; Yamashita, et al. 1985). Finally, for the end-stage of the chondral lesion and irreversible degenerative joint pathology, the standard surgical intervention is total joint arthroplasty.

Whilst each of these treatments are to date the best and often only viable action known to help temporally repair articular cartilage damage they possess many limitations of which the repaired tissue develops more often into fibrocartilage rather than real hyaline

articular cartilage, which although partially successful in alleviating pain in the short run is not a viable long-term solution. This often results again in a degenerative process taking hold thereby requiring continuous long term follow-up procedures of the same type. It is because of these poor outcomes of current surgical strategies, that has promoted medical and regenerative scientists to find alternatives through stem cell-based biomaterial research to develop long-term solutions that could more appropriately heal the defect instead of just temporally fixing it.

1.3.2 Regenerative articular cartilage repair

Before 1994 limitations in repairing articular cartilage damage successfully was limited, until Brittberg et al. (1994) introduced a cell-based therapy in which culture-expanded autologous chondrocytes were transplanted into chondral defect sites through which hyaline-like cartilage formation was achieved, providing the basis from which the concept of cellular based and subsequently biomaterial articular cartilage formation would develop (Brittberg, et al. 1994). Similar to autogenous bone grafting that to date remains the golden standard to heal bone defects clinically (Havers 1692; Ollier 1867; Senn 1889), autologous chondrocyte or cartilage implantation (ACI) has become a commonly utilised orthopaedic surgical technique that can significantly improve the chances of reforming cartilage in articular cartilage defects over a more extended period of time than usual surgical interventions towards articular cartilage defects (Gillogly, et al. 1998; Grande, et al. 1989; Grande, et al. 1987; Pascual-Garrido, et al. 2009; Viste, et al. 2012). However, autologous chondrocyte implantation also has several limitations. Often a cartilage graft when harvested from an articular joint, much like in autogenous bone graft, can cause distinct donor site morbidity, limiting the amount of autologous

chondrocytes material that can be harvested at a given time (Cui, et al. 2009; Gao, et al. 2007). On the other hand, obtaining allografts from other donors pose a severe health risk as there is a danger of either pathogenic transfer occurrence or immunological rejection (Fan, et al. 2013; Gilbert 1998; Nejadnik, et al. 2010).

Moreover, *in vitro* expansion of chondrocytes remains problematic where chondrocyte cellular expansion in culture is limited to a certain number of passages, of which the cells tend to dedifferentiate into fibroblasts terminally (Darling and Athanasiou 2005b; Gosset, et al. 2008; Stokes, et al. 2002), making them unsuitable for use clinically and significantly limiting *in vitro* analyses. Other limitations concerning the ACI procedure are also related to the lack of a viable biomimetic scaffold with multipotent stem cells which together could provide a more balanced physical and biological response necessary to facilitate proper growth and differentiation into hyaline articular cartilage. As such through advances in regenerative tissue engineering , especially stem cell-based research, one could circumvent the shortcomings and limitations of existing therapies to facilitate better healing.

1.4 Stem cells in articular cartilage repair

Stem cell-based therapies over the years has emerged as a great alternative to overcome the poor self-repair capacity of cartilage, as highlighted under the bone induction principle, of an insoluble substratum combined with soluble signal(s) (Reddi 2000; Sampath and Reddi 1981; Urist, et al. 1967), being able to facilitate the formation of *de novo* tissue formation. Similarly to this principle cartilage regeneration utilises chondrocytes or stem cells (soluble signal) combined with a biomimetic biomaterial

(insoluble signal) that facilitates the formation of neo-cartilage tissue *in vitro* and *in vivo* that possesses similar characteristic as actual hyaline articular cartilage (Awad, et al. 2004; Liu, et al. 2010a; Ochi, et al. 2001; Xie, et al. 2012; Ye, et al. 2009).

For cell resources, instead of autologous chondrocytes, studies have focused on mesenchymal stem cells (MSCs), which are considered an alternative cell source for chondrogenic progenitor stem cells due to their excellent capacities at proliferating and possessing the capacity to differentiate into chondrocytes (Grande, et al. 1995; Huang, et al. 2010; Huang, et al. 2014; Morille, et al. 2016; Wakitani, et al. 1994). Thus, adult mesenchymal stem cells from bone marrow, termed bone marrow-derived stem cells (BMSCs), or from adipose tissue, termed adipose-derived stem cells (ADSCs), have been considered as an alternative stem cell, as they equally possess cellular growth kinetics, cell senescence, multi-lineage differentiation and gene transduction efficiency, allowing them to be effectively utilized for generating various specialized cell types, under the correct conditions (Elahi, et al. 2016; Wei, et al. 2013), or tissues for that fact (da Silva Meirelles, et al. 2006). Especially in cartilage tissue engineering BMSCs have been shown to be a fantastic stem cell candidate for research and clinical applications (Deng, et al. 2013; Fortier, et al. 1998; Johnstone and Yoo 1999; Loken, et al. 2008).

Here, in relation to mature chondrocytes which are typically highly differentiated cells, as seed cells, the BMSCs could not only differentiate into the chondrocytes that reform parts of the damaged cartilage tissue layer but could also under the correct conditions reconstruct sub-chondral bone *in vivo* (Bara, et al. 2014; Dwivedi, et al. 2017; Zhou, et al. 2006). However, due to the quantity of viable required BMSCs essential to facilitate such

procedures, necessitating thus often large, invasive and painful autologous bone harvesting procedures resulting in donor site morbidity (Csaki, et al. 2008; Stosich and Mao 2007), alternative stem cell types that can be harvested *en masse* without affecting overall patient homeostasis were necessary. To solve this problem ADSCs were deemed a tremendous viable alternative, as adipose tissue can easily be obtained from beautification liposuction surgeries without any hostile side effects to the patient (Stosich and Mao 2007). ADSCs within the adipose tissue are extremely abundant (Gimble and Guilak 2003) and can easily be isolated to be made to differentiate into multi-lineages (De Ugarte, et al. 2003; Gao, et al. 2007; Winter, et al. 2003; Xie, et al. 2012). Subsequently ADSCs have also been shown to be viable for use in chondrogenesis related experiments, being able to differentiate easily into chondrocytes both *in vivo* and *in vitro* (Fang, et al. 2014; Lu, et al. 2012; Ye, et al. 2009), under the stimulation of TGF- β_3 for chondrogenic induction *in vitro* (Estes, et al. 2010; Ude, et al. 2017). Thus, it is possible to use ADSCs as seed cells to undergo chondrogenic differentiation to engineer cartilage tissue.

The critical issue for stem cells used in tissue engineering is the initiation and control of cellular differentiation where two-dimensional (2D) monolayer conventional culture conditions including the system and serum-supplemented medium methods, tend to cause ADSCs to differentiate into an adipogenic or osteogenic lineage rather than the required chondrogenic lineage (Heng, et al. 2004; Lo Furno, et al. 2016). Therefore, developing a suitable culture technique to direct ADSCs into a chondrogenic lineage is a crucial prerequisite for cartilage defect repair applications utilizing ADSCs. In particular, the culture conditions employed and the physical interactions that occur between the

cells and extracellular matrix (ECM) can exert a profound influence. Environmental factors regulating the shape and alignment of cells, cell adhesion and migration including the build-up of mechanical stresses in the cytoskeleton have all been identified as essential factors that can exert an influence on the chondrogenic differentiation potential of stem cells (Hsu, et al. 2011; Li, et al. 2005; Mahmoudifar and Doran 2010). Typically, the differentiation of stem cells is more suitable when incorporated within a three-dimensional (3D) high-density cell aggregated (spheroid, micromass culture, and pellet culture) cell culture system, now the standard 3D culture systems (Tare, et al. 2005), that allow improved cell to cell interactions similar to those within *in vivo* pre-cartilage condensation process during embryonic cartilage development (Panadero, et al. 2016; Zhang, et al. 2010). However, 3D pellet cell cultures because of an often limited size complicated by weak mechanical properties are unsuitable in the clinical application for the repairing of cartilage lesions (Li, et al. 2005), where biomimetic biomaterial devices replicating specific matrix components have emerged as better alternatives in directing proper matrix formation.

1.5 Biomaterials and cartilage repair

Natural or synthetic based biomimetic scaffolds (biomaterials) designed with nonlinear, inhomogeneous and viscoelastic properties can replicate both the structural and also behavioral characteristics of native of hyaline articular cartilage, providing not only the necessary structural template for the re-formation of new cartilage but also serves as an extracellular matrix substratum that facilitates cellular attachment, proliferation, differentiation to the desired cyto-phenotype thereby ensuring proper integration into the

adjacent the surrounding cartilage tissue defect site (Awad, et al. 2004; Cavallo, et al. 2013; Correa and Lietman 2017; Guilak, et al. 2001).

The type of biomaterial and its specific geometric configuration are key elements, considered in the development of new materials for causing targeted stem cell differentiation into specific tissue types (Ripamonti, et al. 2008; Salim, et al. 2004; Zhang, et al. 2015). As there is a wide range of natural and synthetic biomaterials available, selecting the appropriate biomaterial is crucial (Liu, et al. 2013; Shin, et al. 2003), as the material needs to both provide the necessary cues for cell development and differentiation but also possess excellent biocompatibility so as to integrate flawlessly into the defect site. Several natural biomaterials used for adipose tissue engineering include matrigel, collagen type I matrix, a collagen-chitosan blend or collagen sponges with synthetic biomaterials used for adipose tissue engineering involving polyglycolic acid (PGA) scaffolds, polylactic acid, poly(lactic-co-glycolic acid) and poly(ϵ -caprolactone) (Dahlin, et al. 2014a; Vinatier and Guicheux 2016). The polysaccharide chitosan, a component derived from the exoskeleton of crustacean and insect (Chandy and Sharma 1990; Pugnali, et al. 1988; Younes and Rinaudo 2015) is a copolymer of glucosamine and N-acetyl-glucosamine, obtained by the deacetylation of chitin. It is the most widely used biopolymer in various biomedical applications because of its potential at stimulating hemostasis and accelerating the regeneration of damaged or lost tissues in the process of wound healing (Hoekstra, et al. 1998; Oryan and Sahvieh 2017). Chitosan possesses an excellent ability to form synthetically derived porous structures, generated by freezing and lyophilizing (Madhally and Matthew 1999). It has a hydrophilic surface that enhances cell adhesion, proliferation and differentiation

efficiently attracting fluids and cells to the defect site (Costa-Pinto, et al. 2011). Chitosan has been shown to mimic the natural components of cartilage and possess excellent biocompatibility (Hoffmann, et al. 2009), physicochemical properties including being bioactive and biodegradable making it a good candidate for cartilage tissue engineering (Oryan and Sahviah 2017; Zhang, et al. 2013). When combined with the corresponding stem cell type and or morphogens it could become a viable alternative to other cartilage tissue engineering prospects.

2. Hypothesis of the Study

The hypothesis was that human adipose-derived stem (hADSCs) cells would differentiate into articular matrix forming chondrocytes within pure porous chitosan-based biomimetic scaffolds *in vitro*.

3. Aims and Objectives

Since there are limited studies that have assessed the biocompatibility and tissue engineering capabilities of pure porous chitosan scaffolds with hADSCs, the aim of this study was to evaluate the chondrogenic differentiation but especially the articular cartilage matrix formation potential of human adult ADSCs when these were applied to 1% porous chitosan-based scaffolds (PCSs), within a chondrogenic-simulating environment *in vitro*.

Study Objective 1:

Monitor stem cell survival, proliferation, differentiation and matrix formation capabilities utilizing Live/Dead, Wst-1, Pico-Green and Scanning electron microscopy coupled with immunofluorescent assays respectively, when hADSCs are cultured on 1% PCS in a chondrogenic or standard *in vivo* replicating *in vitro* environment.

Study Objective 2:

Validate that hADSCs do in fact differentiate into articular forming chondrocytes on 1%PCS under standard or chondrogenic culturing conditions, by monitoring key gene expression events in the articular and endochondral bone formation pathways utilizing

quantitative reverse transcription real-time polymerase chain reaction (qRT-PCR) according to the Bustin et al (2009, 2013) MIQE guidelines.

4. Materials and methods

The methods employed in the present study were performed in two phases. Firstly, hADSCs were isolated from the adipose tissue from donor patients and cultured up to passage 4 after which the cellular attachment, chondrogenic differentiation and proliferation potential including the corresponding matrices that were secreted by the cells into the macroporous spaces of 1% porous chitosan scaffold was assessed (**Objective 1**) and validated (**Objective 2**).

4.1 1% Porous chitosan constructs (PCS)

The 1% PCSs used in this study were custom produced by the Advanced Materials Research Center of the Friedrich-Baur BioMed Center in Bayreuth of Germany. Briefly, first porous sponges were made by lyophilization of glutaraldehyde-crosslinked 1% weight to volume (w/v) chitosan hydrogels as described in (Hoffmann, et al. 2009). Here, chitosan with a 95% degree of deacetylation (Heppe Medical, Halle) was dissolved at 2% w/v. in 0.1N hydrochloric acid at pH1. Using 1N sodium hydroxide, the pH was adjusted to 5 by careful, dropwise addition under constant stirring on a magnetic stirrer (Thomas Scientific, NJ, USA) platform. Hydrogels were formed by mixing 1 ml of chitosan solution with 1 ml aqueous 1% glutaraldehyde solution (Sigma-Aldrich, St. Louis, USA) in forms with 15 mm in diameter. After gelation, the samples were frozen at -32°C using polystyrene insulation to control the freezing rate. Frozen samples were freeze-dried at -50°C under vacuum using an Alpha 1-4 LD system (Christ, Lagos State, Nigeria). The

dry scaffolds were trimmed on both ends to a final height of 8mm with a microtomic blade. Chitosan scaffolds were then gamma-sterilized at ca. 27 kGy. Quality check to ensure correct morphological scaffolds was performed using a VHX-5000 3D digital microscope (Keyence, Osaka, Japan) and software VHX-5000 Ver. 1.6.1.0 / System Ver. 1.04 (Keyence, Osaka, Japan). The microstructure of the scaffolds was captured utilizing a Zeiss EVO LS 10 scanning electron microscopy (SEM) (Zeiss, Oberkochen, German).

4.2 Isolation and culture of human adipose-derived stem cells (hADSCs)

Human ADSCs were isolated, as previously described (Bondarava, et al. 2017), from subcutaneous adipose tissue that was acquired from the Biobank of the University Hospital of Munich Germany which operates in accordance to the European Union compliant ethical and legal framework of the Human Tissue and Cell Research Foundation (<http://www.htcr.org>). The research was approved by the Human Ethics Committee of the Faculty of Medicine (#315-13) at the University of Munich and the Bavarian State Medical Association. Briefly, harvested adipose tissue was rinsed with phosphate buffered saline (PBS) containing 180 IU/ml penicillin/streptomycin and 0.75 µg/ml amphotericin B (Biochrom, Berlin, Germany), after which the tissue was cut into small pieces and digested by 0.2 % collagenase A solution (Sigma-Aldrich, St. Louis, USA) in DMEM (Gibco, Waltham, MA, USA) at 37°C. Then, 15% fetal calf serum (FCS; Sigma-Aldrich) supplemented culture medium was added, after which the mixture was resuspended, filtered through 100 µm sieves and centrifuged at 400 x g for 10 minutes at room temperature (RT). The pellet containing hADSCs was resuspended with fresh growth medium (DMEM, 15% FCS, 60 IU/ml penicillin/streptomycin), seeded in a T-75

culture flask and cultured at 37°C with 5% CO₂ for 24 hours. Subsequently, the adhered cells were washed with PBS and 20ml of fresh growth medium was added. The medium was replaced every 3 days. Human ADSCs used in this study were used at passage 4.

4.3 Cell seeding onto 1% PSCs and *in vitro* chondrogenic differentiation

The dry chitosan scaffolds were placed carefully in a 12-Nunc well plate (Thermo Fisher Scientific, Waltham, MA, USA) and covered with 2ml normal growth medium consisting of high-glucose DMEM 4.5 g/L D-glucose, 110 µg/ml Pyruvate (Gibco) supplemented with 10% FCS and 60 IU/ml penicillin/streptomycin. Scaffolds were then incubated at 37°C with 5% CO₂ for 6 hours after which the medium was changed and left to incubate overnight. Human ADSCs (~90% confluent) were then digested with trypsin/EDTA, counted and resuspended at a concentration of ~1x10⁷/ml. To seed the cells on the chitosan scaffolds, the old medium was removed and 100 µl of cell suspension was pipetted evenly onto the surface of the devices. Scaffolds with cells were then incubated at 37 °C at 5% CO₂ for 1h to allow for cell attachment to the device, whereupon 2ml of normal growth medium was added to each well and incubated overnight. The following morning (**Day1**), the cell-seeded scaffolds were transferred into either normal growth medium (**Normal + Scaffold** or “**NS**”; **n=9**) or chondrogenic medium (**Chondrogenic + Scaffold** or “**CS**”; **n=9**). Chondrogenic medium consisted of normal growth medium supplemented with 10 ng/ml recombinant human TGF-β₃ (R&D Systems, Minneapolis, MN, USA), 100nM dexamethasone (Sigma-Aldrich), 50ug/ml L-ascorbic acid-2-phosphate (Sigma-Aldrich), 40ug/ml L-proline (Sigma-Aldrich) and ITS +1 (Sigma-Aldrich; final concentrations: 10 mg/L insulin, 5.5 mg/L transferrin, 4.7 µg/ml linoleic acid, 0.5 mg/ml bovine serum albumin and 5 µg/L selenium). The cell-seeded constructs

cultured with normal growth medium (**NS**) were considered as the scaffold control group. Samples were cultured for 7, 14, and 28 days and medium was replaced every 3days.

4.4 Pellet culture and chondrogenic differentiation

Pellet culture was used as comparable, scaffold-free 3D culture control (Estes and Guilak 2011), to investigate both scaffold and culture medium influence on stem cell differentiation and matrix formation. Human ADSCs from the fourth passage were resuspended at a concentration of 2.5×10^5 cells per ml in normal growth medium (see above). Two milliliters of the cell suspension containing 5×10^5 hADSCs were then pipetted into a 15 mL sterile polypropylene conical tube and centrifuged under the speed at $500 \times g$ for 5min to allow for 3D cell pellet formation. The 3D pelleted cells were then incubated overnight at 37°C with 5% CO_2 in Eppendorf tubes with loosened caps to permit gas exchange. Spheroid aggregates formed at the bottom of each tube. The following day (**Day1**), the culture medium was replaced with 2ml of fresh growth medium (**Normal + Pellet** or "**NP**"; **n=9**) or chondrogenic medium (**Chondrogenic + Pellet** or "**CP**"; **n=9**) carefully so as not to resuspend the cell pellet. The 3D pellet medium was changed every 3 days and 3D cell pellets were cultured for 7, 14, and 28 days prior to harvest and processing for analysis. Cells cultured in normal growth medium were used as the pellet control group.

4.5 Scanning electron microscopy (SEM)

In order to visualize the matrix development progression on the scaffolds, one device was randomly chosen and cultured for 1, 7, 14 and 28 days. Upon harvest, the sample was washed with PBS and fixed in 2.5% glutaraldehyde in PBS overnight at 4°C . The

construct was then stained with 1% osmium tetroxide, dehydrated in a graded series of alcohols and finally dried using the critical point drying method after which it was coated with gold. The samples were examined with an EVO LS 10 SEM at an accelerating voltage of 20 kV (Zeiss).

4.6 Cell Viability and Proliferation assay

Viability and proliferation of hADSCs within chitosan based scaffolds was evaluated utilizing a water-soluble tetrazolium reagent (WST-1, Roche, Penzberg, Germany) in combination with Quant-iT™ PicoGreen dsDNA Kit (Invitrogen, Life Technologies, USA) at day 1 and subsequently at day 7, 14, or 28. Briefly, hADSCs-seeded scaffolds were transferred to a new 24-Nunc well plate, washed twice with PBS, after which 0.5ml fresh normal growth medium containing WST-1 at 10:1 (v/v) was added to each well and incubated for 2 hours at 37°C at 5% CO₂. The absorbance of the WST-1/medium mixture was read at 450 nm using a Synergy HT microplate reader with Gen 5 2.03 software (BioTek, Bad Friedrichshall, Germany) in a 96-well plate. The same scaffolds were used for the PicoGreen dsDNA Assay. Here the samples were washed twice with PBS. According to the manufacturer's protocol, the cells were lysed from the scaffold and DNA standards were mixed with TE-buffer and subsequently with Quant-iT PicoGreen dsDNA reagent. The samples were excited at 480 nm and the fluorescence emission intensity was measured at 520 nm using a Synergy HT microplate reader with Gen 5 2.03 software (BioTek).

4.7 Cell survival in the scaffold

The effect of cultivation in chitosan sponges on cell survivability in relation to the number of dead cells in chondrogenic differentiation medium was studied using a LIVE/DEAD Viability/Cytotoxicity Kit (Invitrogen). At day 1, 7, 14 and 28 the cell-scaffold constructs were rinsed with PBS and incubated in a staining solution containing Calcein AM and Ethidium homodimer-1(EthD-1) at room temperature for 30 min. After washing with PBS the constructs were then examined under a Axio Vert.A1 Inverted fluorescence microscope (Zeiss). Healthy cells or dead cells fluoresce green or red, respectively (Yang, et al. 2008).

4.8 Histological analysis and Immunofluorescence staining

After 7, 14 and 28 days of culture the cell-scaffolds and 28 day 3D cell pellets were harvested and specimens were then fixed in 4% paraformaldehyde for 30 min at room temperature. The 1% chitosan-based scaffold specimens with cells were then dehydrated through a graded series of alcohols into paraffin, whereas the 3D cell pellet cultures were embedded in a Tissue-Tek O.C.T.™ compound (Sakura Finetek, Staufen, Germany) and frozen in liquid nitrogen. Following this, 10 µm thick sections were cut using either a Microtome (Leica, Wetzlar, Germany), for paraffin specimens, or a CM 3050 cryomicrotome (Leica), for the cryogenic embedded specimens. To visualize tissue morphology and cartilage matrix formation, sections were stained with either, hematoxylin and eosin (H&E) for morphological evaluation(Landini and Perryer 2009), or Alcian blue at ph 2.5 for glycosaminoglycan (GAG) content formation(Green and Pastewka 1974). All stained sections were analyzed with a PreciPoint M8 Digital Microscope & Scanner (PreciPoint GmbH, Freising, Germany).

To determine the quality of the matrix composition secreted by cells in chitosan-based scaffolds within the **CS** and **NS** groups, immunofluorescence staining for collagen I, collagen II and aggrecan was performed. Briefly, paraffin sections were incubated with primary antibodies (all from Abcam, Cambridge, UK) for either collagen type I (1:300; Cat# ab34710), collagen type II (1:200; Cat# ab34712) or aggrecan (1:300; Cat# ab3778) at 4°C overnight. The antibodies were diluted with antibody dilution buffer (DCS, Germany). For negative controls, the first antibody was omitted. For positive control, use the hyaline cartilage section from the normal human knee to ensure the antibody was working correctly. The slides were then incubated with the conjugated secondary antibody (Abcam, Cambridge, UK) for 1 h at room temperature. Nuclei of cells were then stained for 8min with Hoechst 33342(Life Technologies, Carlsbad, USA), which will show blue dye under the inflorescence microscopy. The slides were mounted with Fluoromount W (Serva Electrophoresis, Heidelberg, Germany), air-dried and stored in darkness at 4 °C. Fluorescence microscopy was then performed with a Zeiss Axioskop 40 equipped with appropriate filter sets and AxioCam MRc 5 (Carl Zeiss, Munich, Germany). Images were obtained with Axio Vision, Rel. 4.9 (Carl Zeiss, Munich, Germany). Exposure time was kept constant for the samples where fluorescence intensity was to be compared.

4.9 QRT-PCR according to Bustin's MIQE Guidelines

In order to generate the most accurate gene expression profiles thereby reflecting whether articular cartilage formation was indeed occurring within chitson-based scaffolds seeded with hADSCs the quantitative reverse transcription real-time polymerase chain

reaction procedures was performed in accordance to the strict guidelines as set out by Bustin et al 2009 and 2010.

4.9.1 Gene primer design and optimisation

Endochondral bone formation and articular cartilage gene markers together with reference genes, reference genes known to be suitable for the normalization of qRT-PCR expression studies that focus on those with a standard deviation of the average amplification threshold (Cq) of less than 1 across 35 in human cell (Dheda, et al. 2004; Warrington, et al. 2000), were custom designed, utilising the relevant mRNA sequences *Homo sapiens*, from GenBank (<http://www.ncbi.nlm.nih.gov/genbank/>), together with PrimeQuest in conjunction with OligoAnalyzer 3.1 on the IDT website (<https://eu.idtdna.com/site>). The specificity of the designed primers was confirmed through the use of the Basic Local Alignment Search Tool program on Pubmed Central (<https://blast.ncbi.nlm.nih.gov/Blast.cgi>).

Eight potential forward and reverse primers of 8 reference genes and six endochondral osteogenic and chondrogenic relative target genes were designed. For the 8 reference *TATA-binding protein (TBP)*, *glyceraldehyde 3-phosphate dehydrogenase (GAPDH)*, *RNA 28S ribosomal 4 (RNA28S4)*, *RNA polymerase II subunit e (POLR2e)*, *ribosomal protein lateral stalk subunit P0 (RPLP0)*, *succinate dehydrogenase complex flavoprotein subunit A (SDHA)*, *actin beta (ACTB)*, *ribosomal protein L13a (RPL13a)* were designed whilst the 6 endochondral bone and articular cartilage formation genes included in this study were *aggrecan (ACAN – articular cartilage marker)*, *collagen type II (COL2A1 – articular cartilage marker)*, *collagen type X (COL10A1 – endochondral marker)*, *collagen*

type I (COL1A1 – endochondral marker), SOX9 (articular cartilage and endochondral marker) and cartilage oligomeric matrix protein (COMP – cartilage marker) (Table 1).

Generated gene primers were optimized using a standard temperature gradient run to determine the optimal range of primer annealing temperatures. Each reaction contained 25ng cDNA (from chondrogenic differentiated hADSCs), with 2x FastStart Essential DNA Green Master (Roche, Basel, Switzerland) and 10 µM of each primer (**Table 1**) in a final reaction volume of 10 µl. Runs were performed in a LightCycler® 96 thermocycler (Roche, Basel, Swiss), with thermocycling parameters including a pre-incubation of 3 min at 95°C, followed by a three-step amplification program of 40 cycles consisting of a denaturation, annealing and extension step set at 95°C for 10 s, 55 to 65 °C for 15s and 72°C for 30s, respectively. A melt curve was included in each run to confirm amplification of a single product. After PCR amplification wells identified with positive amplicons, and therefore generating a valid temperature range at which primers function optimally, were purified with the MinElute PCR Purification Kit (Qiagen, Crawley, UK), according to the manufacturer's instructions and analyzed, after Sanger sequencing (GATC Biotech, Cologne, Germany) utilizing BLASTn against the GenBank database to validate primer reference gene and target gene sequences amplification specificity.

4.9.2 cDNA standardization for qRT-PCR

Too much or too little cDNA can prevent proper gene amplification within a reaction. At the correct quantity of cDNA one can also maximize the number of genes one can analyze per sample making cDNA standardization a necessary requirement to facilitate a broad spectrum analysis of genes within an experiment. As such the optimum cDNA

quantity to be used per qRT-PCR using a standard curve was utilized to determine this. A 2x dilution gradient of cDNA amounts, specifically 40 ng, 20 ng, 10ng, 5 ng, 2.5ng and 0ng, was utilized to generate the standard curve in relation to the amplification threshold (Cq). PCR reactions were carried out in 96-well plates in duplicate. The PCR reactions were performed using a qRT-PCR LightCycler® 96 Instrument (Roche, Basel, Swiss), where the total volume per reaction was 10µl, containing 10µM of each reference primer (**Table 1**), the corresponding diluted cDNA and 2x FastStart Essential DNA Green Master (Roche). The thermocycling procedure included a pre-incubation of 3 min at 95°C, followed by a three step amplification program of 40 cycles consisting of a denaturation, annealing and extension step set at 95°C for 10 s, 60 °C for 15s and 72°C for 30s, respectively. A melt curve was included in each run to validate product amplification. Standard curve determined that an optimal cDNA amount of 10ng per reaction was the most appropriate to utilize in the qRT-PCR analysis.

4.9.3 Stability and quantity of reference primers (GeNorm)

A GeNorm analysis was performed to determine which of the 8 reference genes were the most stably expressed within the experiment and how many of these reference genes were necessary to facilitate proper normalization in relation to the test genes. All treated and control groups within the experiment were incorporated into the GeNorm validation process including hADSCs fresh (endogenous baseline control) PCR reactions were carried out in 96-well plates in duplicate utilizing a qRT-PCR LightCycler® 96 Instrument (Roche) with a total reaction volume of 10µl, that contained 10µM of each reference primer (**Table 1**), 10 ng of cDNA and 2x FastStart Essential DNA Green Master (Roche). Thermocycling parameters had a pre-incubation step of 3

min at 95°C, followed by a three-step amplification program of 40 cycles consisting of a denaturation, annealing and extension step set at 95°C for 10 s, 60 °C for 15s and 72°C for 30s, respectively. A melt curve was included in each run to validate product amplification. Generated data was then inputted into GeNorm (<http://medgen.ugent.be/wjvdesomp/genorm/>) using the relative quantities based on the comparative threshold cycle (Cq) method (VanGuilder, et al. 2008). The statistical tools used by GeNorm were used to assess the expression stability of the candidate reference gene using the M-value, which refers to the average pairwise variation between each reference gene and the other reference genes. A gene with $M < 1.5$ is considered as a stable reference gene. Subsequently, the pairwise variation (V-score) was determined which indicates the optimal number of reference genes to use for the cell or tissue type to generate realistic and accurate relative quantitative gene expression data (Bustin, et al. 2009; Dolgin 2017; VanGuilder, et al. 2008). The value of $V_{n/n+1}$ under 0.15 indicates that no additional reference genes are required for normalization (VanGuilder, et al. 2008).

4.9.4 qRT-PCR

QRT-PCR was performed to determine the relative expression of the chondrogenic genes, *aggrecan (ACAN)*, *collagen type II (COL2A1)*, *cartilage oligomeric matrix protein (COMP)*, *SRY-box 9 (SOX9)* with *collagen type I (COL1A1)* and *collagen type X (COL10A1)* being included to determine if cartilage matrix development was purely articular or progressing towards an endochondral ossification lineage. After 7, 14 and 28 days, total RNA was isolated using a modified RNA Trizol extraction procedure (Chomczynski and Mackey 1995). Briefly, 1 ml Trizol (Invitrogen) was added to cell

material after which chloroform (Sigma-Aldrich) was added to permit separation of the RNA from the proteinaceous material. After centrifugation, the aqueous RNA containing phase was transferred to a fresh tube where the RNA was then precipitated by adding Isopropanol (Sigma-Aldrich). After incubating at RT for 10 min, the samples were centrifuged at the speed of 16000 rpm overnight at 4 °C, upon which RNA pellets were then washed with 75% Ethanol (Merck, Billerica MA, USA) and permitted to dry briefly to prevent alcohol contamination. Following drying, total RNA was resuspended in 32 µl RNase free water (Gibco) and assessed the purity and concentration of the RNA using a NanoDropTMLite spectrophotometer (Thermo Scientific) and quality assessed with a Bioanalyzer 2100 (Agilent Technologies). Finally, approximately 1 µg of RNA was reverse transcribed into complementary DNA (cDNA) utilizing the QuantiTect Reverse Transcription cDNA Synthesis Kit (Qiagen, Germany).

QRT-PCR was then performed in duplicate, using the FastStart Essential DNA Green Master (Roche, Basel, Switzerland) on a Light Cycler 96 thermocycler (Roche, Basel, Swiss). Each reaction mixture contained 10 ng cDNA, 10 µM of each primer (**Table 1**), 2x FastStart Essential DNA Green Master and RNase-free water to a final reaction volume of 20 µl. From section **4.9.3 of the Materials and Methods Section**, GeNorm analysis identified that in order to generate realistic gene expression data four reference genes had to be utilized, of which the most stably expressed were *TATA sequence binding protein (TBP)*, *β-actin (ACTB)*, *ribosomal protein lateral stalk subunit P0 (RPLP0)* and *RNA polymerase II subunit E (POLR2e)*. PCR thermocycling conditions included a 3min pre-incubation at 95°C, followed by a three-step amplification program of 40 cycles consisting of a denaturation, annealing and extension step set at 95°C for 10 s, 58 °C for

15s and 72°C for 30s, respectively. Relative expression between samples of the six target genes was normalized to the four reference genes using the qbase+ software (<https://www.qbaseplus.com>). Data was further normalized to unaltered hADSCs in monolayer which was the baseline to which experimental groups were compared.

Table 1. Gene primers used for optimization

	Gene	Forward primer (5'- 3')	Reverse primer (3' - 5')	Accession Nr.	Amplicon Size (bp)
Test genes	<i>COL2A1</i>	GCCCAGTTGGGAGTAAGT	CACCAGGATTGCCTTGAA	NM_001844.4	106
	<i>COL1A1</i>	GCTGGTCCCTCCAGGTGAA	GGGGACCAACAGGACCA	NM_000088.3	159
	<i>COL10A1</i>	TGGCCTGCCTGACTTTA	AATGTCCAGCTCACTGGA	NM_000493.3	151
	<i>ACAN</i>	ACCCAAGGACTGGAATCT	CCTGATCCAGGTAGCCTT	NM_001135.3	149
	<i>COMP</i>	TGCACCGACGTCAACGA	CCGGGTGTTGATGCACA	NM_000095.2	231
	<i>SOX9</i>	GTGGCTGTAGTAGGAGCT	GCGAACGCACATCAAGA	NM_000346.3	155
	reference genes	<i>SDHA</i>	CTTCCTTGCCAGGACCTA	GGCGTATCGCTCCATAAAC	NM_001330758.1
<i>POLR2e</i>		CTATCTGGTGACCCAGGA	CTGCAGAAACTGCTCCA	J04965.1	322
<i>TBP</i>		CACTTCGTGCCCGAAAC	GCCAGTCTGGACTGTTCT	BC110341.1	121
<i>ACTB</i>		CTGCCCTGAGGCCACTC	GTGCCAGGGCAGTGAT	NM_001101.3	197
<i>RPL13a</i>		CTTTCCTCCGCAAGCGG	GTCCGCCAGAAGATGCG	NM_012423.3	159
<i>RNA28S4</i>		GCGGCCAAGCGTTCATA	CCTGTCTCACGACGGTCTAA	NR_145822.1	143
<i>GAPDH</i>		CATGGGTGTGAACCATGA	TGTCATGGATGACCTTGG	BC083511.1	104
<i>RPLP0</i>		CAACCCAGCTCTGGAGA	CAGCTGGCACCTTATTGG	BC001834.2	116

4.10 Statistical analysis

Data from triplicate cultures are presented as means \pm standard deviation (SD, n=9) for the results of WST-1, PicoGreen and qPCR. Qbase+ software was used to analyze the data from qPCR. Microsoft Excel and Prism 5.02 software (GraphPad Software, San Diego, USA) were used for analyzing the data. The Students' T-test was used for comparing groups of data. Values for $p < 0.05$, $p < 0.01$ and $p < 0.001$ were considered significant, highly or extremely significant, respectively. Statistical significance is indicated by * for $p < 0.05$, **for $p < 0.01$ and ***for $p < 0.001$.

5. Results

5.1 Characterization of porous chitosan scaffold and seeding with differentiated hADSCs

The chitosan scaffolds appeared as a soft and highly porous spongy-like disk (**Fig. 1A**). SEM micrographs showed that the scaffolds contained pores of approximately 100-200 μm in diameter. The magnified view of the pores was relatively uniform and had irregular morphology (**Fig. 1B**). The scaffold structure appeared different after cultivation in medium, which might be due to drying during SEM preparation (**Fig. 1C**). Once scaffolds had been seeded with hADSCs and cultured *in vitro* in the chondrogenic medium for 1 day, SEM analysis showed that the cells attached to scaffolds (**Fig. 1D-F**). At day 7, abundant and fibrous matrix had been secreted into the porous structures of the sponges (**Fig. 1G-I**). At day 14, cells in chondrogenic medium continued producing abundant ECM not only on the surface of the scaffold (**Fig. 1J, K**) but also in its inner pores (**Fig. 1L**). With cartilage formation being detectable by day 28, ECM covered all porous spaces and the inside (**Fig. 1 M-O**) of the devices, demonstrating superior scaffold properties of the chitosan sponges.

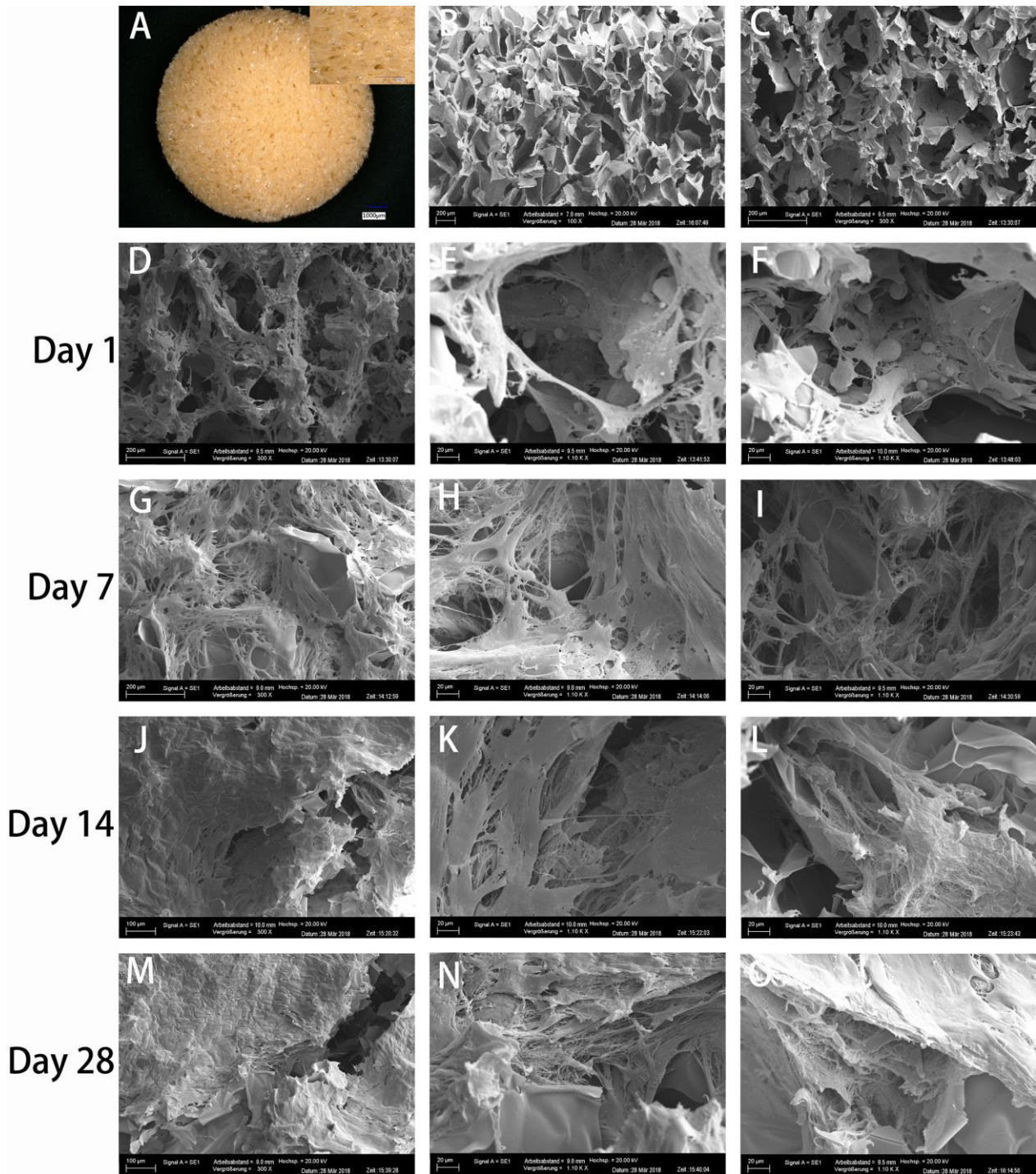


Figure 1. Scanning electron microscopy images (**B-O**) of chitosan scaffolds at different time points in culture. (**A**) The spongy-like topography of non-cultured pure chitosan scaffolds discs in the absence of medium (**B**) possess a rigid microstructural environment that upon addition of medium (**C**) are seen transforming into a geometrical configuration that favors cellular

attachment (**D**), which through chondrogenic medium with hTGF- β_3 and hADSCs already shows minor extracellular matrix deposition after 24h (**D-F**). Human ADSCs in chondrogenic medium quickly and efficiently are observed to be depositing substantial amounts of a collagenous fibrous matrix at day 7 (**G-I**) filling up the microporous structures of the chitosan scaffolds that is aggregating into a woven fibrous structure by day 14 (**J-L**) indicative of cartilage formation. (**M-O**) By day 28 microstructures can no longer be detected by SEM but are seen to be nearly completely covered by extracellular matrix that stains positive for Alcian Blue (GAG). Magnifications were set at 100x (**B**), 300x (**C, D, G, J, M**), 1.10Kx (**E, F, H, I, K, L, N, O**).

5.2 Viability and proliferation of hADSCs on chitosan scaffolds

In order to evaluate cell viability on the hADSCs-seeded scaffolds and to determine proliferation, a WST-1 test in combination with PicoGreen assay was performed 24 hours after cell seeding and subsequently after 7, 14 and 28 days of *in vitro* incubation. Both values increased progressively over the 28 days incubation period indicating a steady increase of cells in all experimental groups, with a marked decrease in slope after 15 days indicating the onset of differentiation (**Fig. 2**). The cell cultures on the scaffolds showed significantly higher viability at all-time points of incubation with a significant difference between **NS** and **CS** groups, chondrogenic medium having stimulated stronger growth and cellular activity (**Fig. 2 A**). Similar results were obtained by PicoGreen dsDNA assay (**Fig. 2 B**). After 14 and 28 days, values were significantly higher than at day 7 for **NS** and **CS** groups (**Fig. 2 A**). After 14 days, proliferation slowed down, a typical process attributed to a change towards differentiation of the cell masses. At that time point, chondrogenic (**CS**) cultures had already reached a higher cell number (**Fig. 2 B**), which was maintained towards 28 days while metabolic activity continued to increase (**Fig. 2 A**).

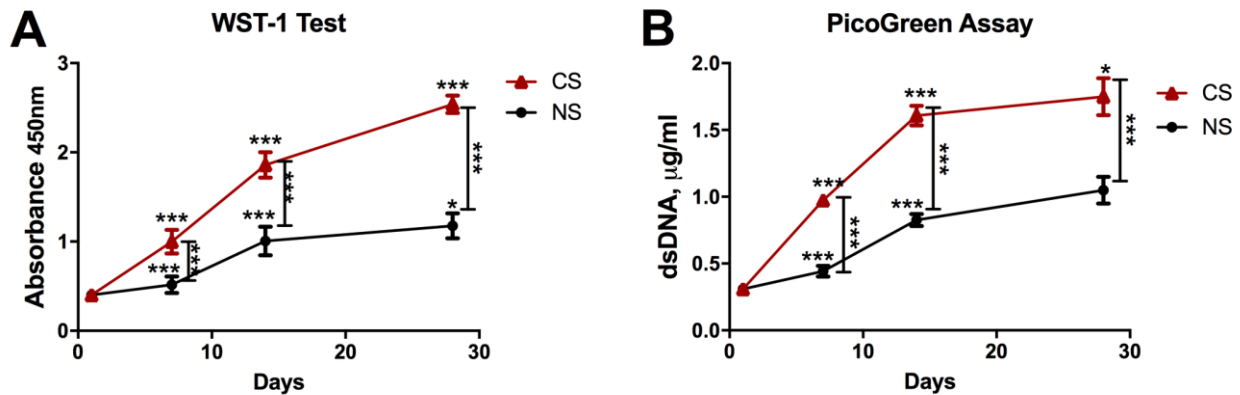
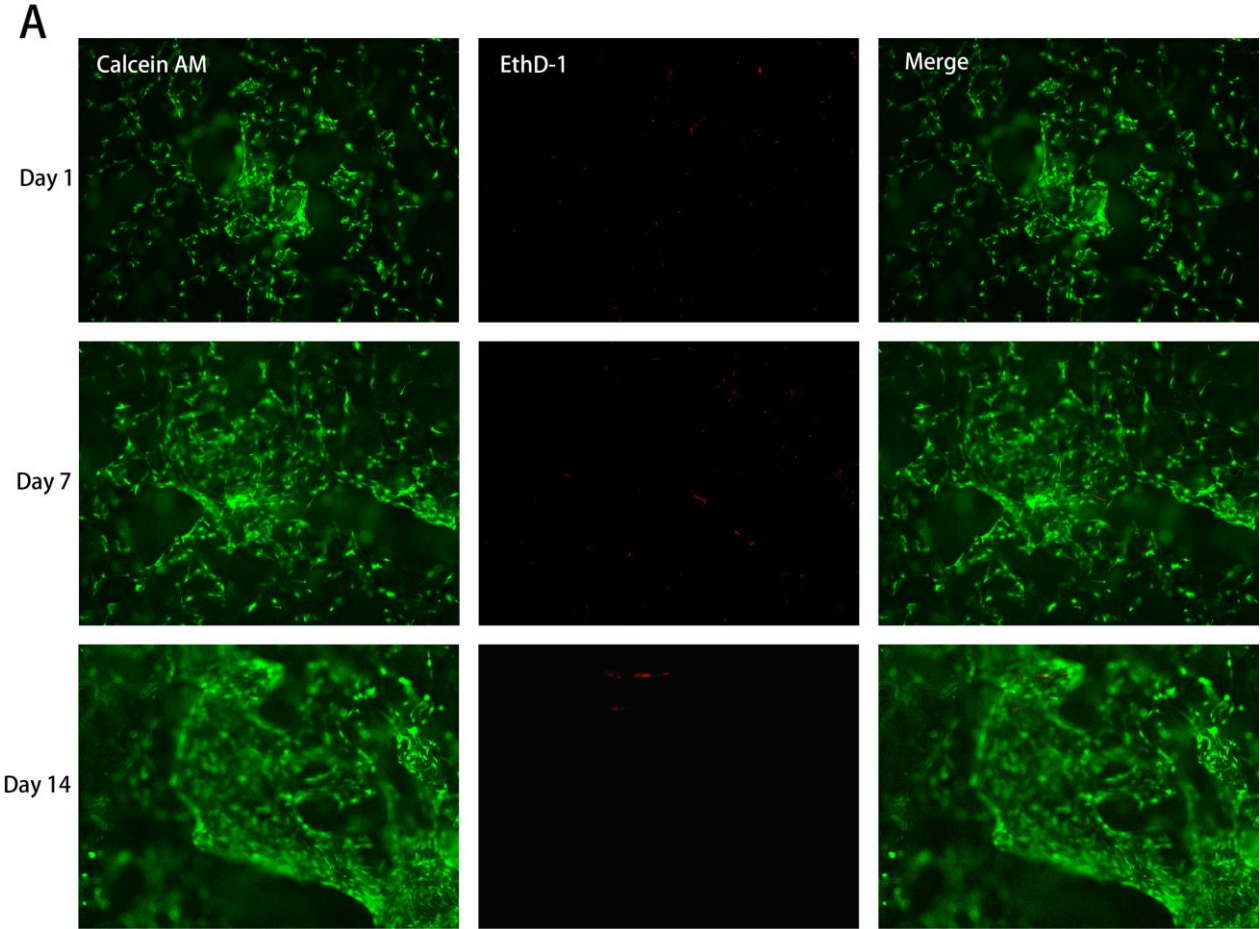


Figure 2. (A) WST-1 (cell viability) and (B) PicoGreen (cell proliferation) assays for hADSCs on chitosan scaffolds cultured with normal (NS) or chondrogenic (CS) medium. The chitosan scaffolds are seen promoting stem cell proliferation and supports cell integrity over the 28 day culturing period under the NS conditions, which through the addition of chondrogenic medium with hTGF- β_3 is significantly increased (CS). The level of significance was set as * for $p < 0.05$, ** for $p < 0.01$, *** for $p < 0.001$.

5.3 Cell survival with Live/Dead Assay in porous chitosan scaffolds

At 1, 7 and 14 days post seeding, cell survival and proliferation in scaffolds treated with chondrogenic differentiation medium (CS) or normal medium (NS) were demonstrated by using live/dead staining. Human ADSCs are attaching to the chitosan and proliferating rapidly on the surface of the scaffolds with high viability over time in both CS (Fig. 3) and NS groups (Fig. 3B), but cells in the CS group proliferated more quickly and formed denser layers than in the NS group. At day 1 post seeding, viable cells were observed on the surface and interior of the constructs including several dead cells (Fig. 3A, B). The viability of the cells was consistent and was observed to increase slightly

from day 1 to 14, with only occasional dead cells, indicating that the chitosan is suitable for *in vitro* cultivation of hADSCs.



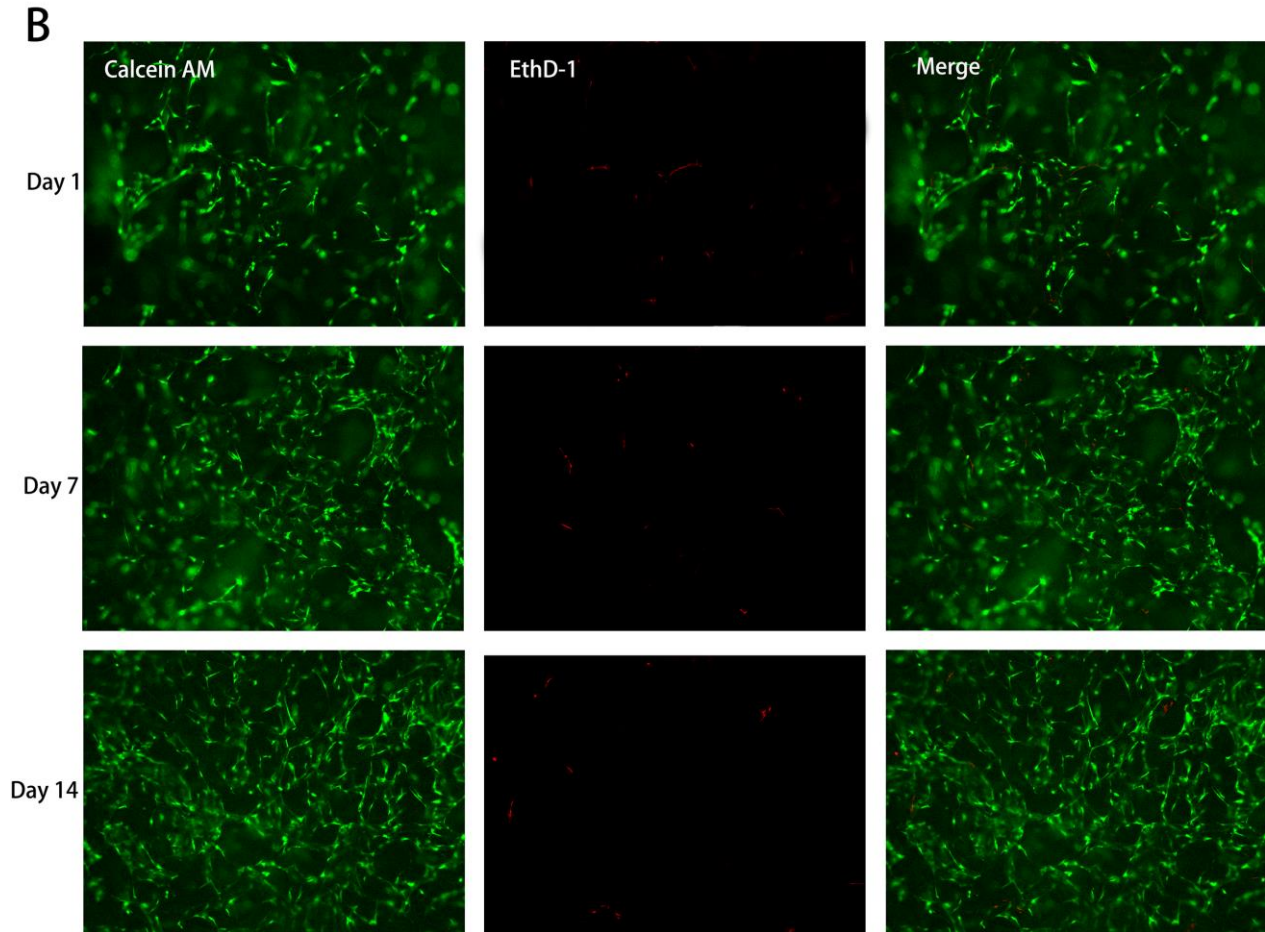


Figure 3. Fluorescent microscopy images of the Live/dead cell survival assay. Living cells fluoresce **green** and dead cells fluoresced **red**. Miniscule or no cell death (EthD-1 images) could be detected in both normal (**B**) and chondrogenic medium (**A**) for chitosan scaffolds groups with hADSCs at day 1, 7 and 14. Living cells (Calcein AM images), on the other hand, remained fully intact as the culturing period increased in which living cells are seen to become more abundant by day 14 after initially seeding the bioreactors with hADSCs.

5.4 Histology analyses of chitosan scaffold culture

Hematoxylin and Eosin (H&E) staining (**Fig.4**) revealed that hADSCs were proliferating more and more evenly distributed in chitosan sponges in chondrogenic medium (**Fig.4D-F**) compared to the normal medium group (**Fig.4A-C**). Moreover, cell density continued

to increase with culture time with round chondrocyte-like cells embedded in ECM being observed at day 28 days of culture (**Fig.4F**).

Alcian blue staining (**Fig.5**) revealed that the density of glycosaminoglycan (GAG) in the matrix formed by the cells was increasing as the culture period progressed in the chitosan with the chondrogenic medium group (**Fig.5 D-F**) here as limited cartilaginous matrix could be seen in the normal medium scaffold treatment group (**Fig.5 A-C**).

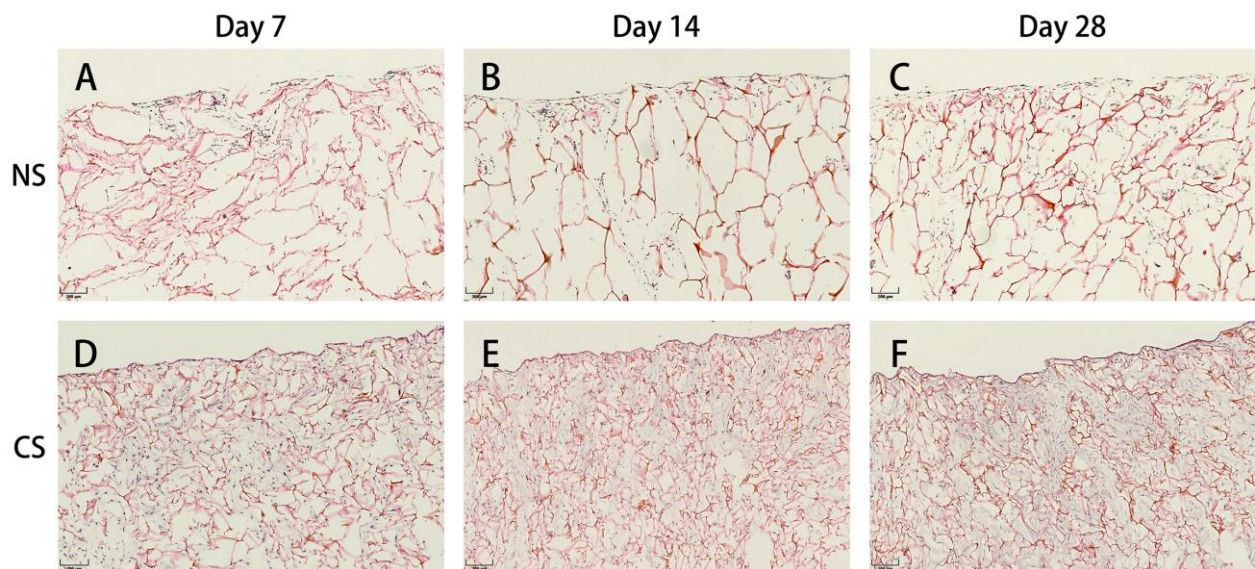


Figure 4. H&E staining to monitor cellular tissue density and distribution of hADSCs in chitosan scaffolds cultured with either normal (**NS**) (**A-C**) or chondrogenic medium (**CS**) (**D-F**), after 7 (**A, D**), 14 (**B, E**) and 28 (**C, F**) days *in vitro*. Substantial cellular and extracellular connective tissue formation is observed as the culturing period increased, with hADSCs/chondrocytes migrating from their initial seeding into the microporous structure of the chitosan devices. Substantially more cellular and connective tissue formation can be observed in the **CS** group (**D, E, F**) than in the **NS** group (**A, B, C**) highlighting the proliferative power of hTGF- β_3 on cell mitosis.

Magnification 40x (Bar scales: 200 μ m).

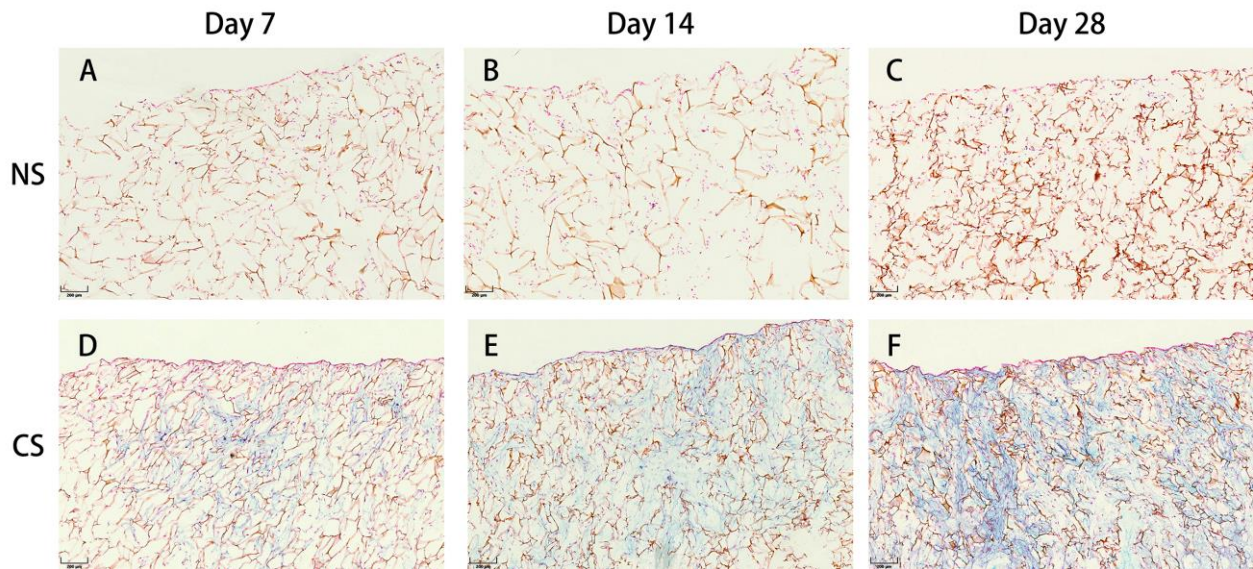


Figure 5. Alcian blue staining for GAG in chitosan scaffolds seeded with hADSCs cultured in either normal (**NS**) (**A-C**) or chondrogenic medium (**CS**) (**D-F**) after 7, 14 and 28 days. Limited or no GAG deposition was observed within the **NS** group. In the **CS** cultured chitosan scaffolds with hADSCs, GAG formation was readily seen even by day 7 (**D**), with the cartilage proteoglycan deposition increasing substantially by day 28 (**F**). This indicates that hADSCs differentiated more quickly in the **CS** than **NS** group, directed by the hTGF- β_3 in the medium. Magnification 40x (Bar scales: 200 μ m).

5.5 Pellet Culture results and histology analyses

After 4 weeks, the chondrogenic pellets were larger and rounder than control pellets and also had a shiny white appearance macroscopically (**Fig. 6**).

H&E staining of **CP** (**Fig.7B**) showed a change in cellular morphology towards a chondrocyte phenotype where larger round chondrocyte-like cells encapsulated in lacunae were seen compared to control pellets (**NP**) (**Fig.7A**), which appeared to have a more fibroblastic morphology. The positive Alcian blue stain observed in the **CP** (**Fig.7D**)

was only weakly detected in the **NP** group (**Fig.7C**). In chondrogenic pellets, in homogenous matrix formation was observed, with several nodules lacking Alcian blue and regions with dense cell masses, which appear partly elongated, while Alcian blue positive regions have a much lower cell/matrix ratio (**Fig.7D**)

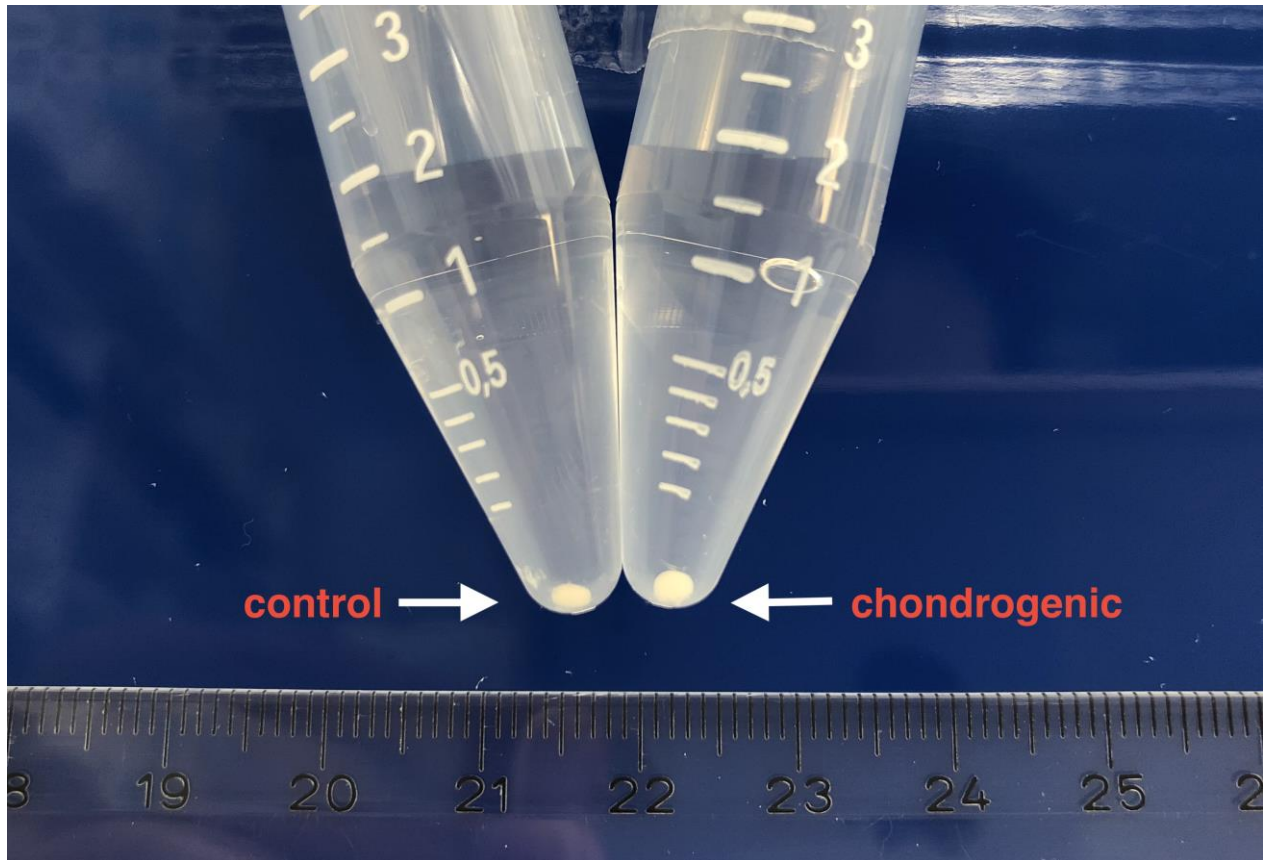


Figure 6. Macroscopic image of pellet cultures in control and chondrogenic media at 4 weeks. A comparative image showing pellets cultured in control vs chondrogenic media shows a distinct difference in size at 4 weeks between the larger chondrogenic pellets and the smaller control pellet.

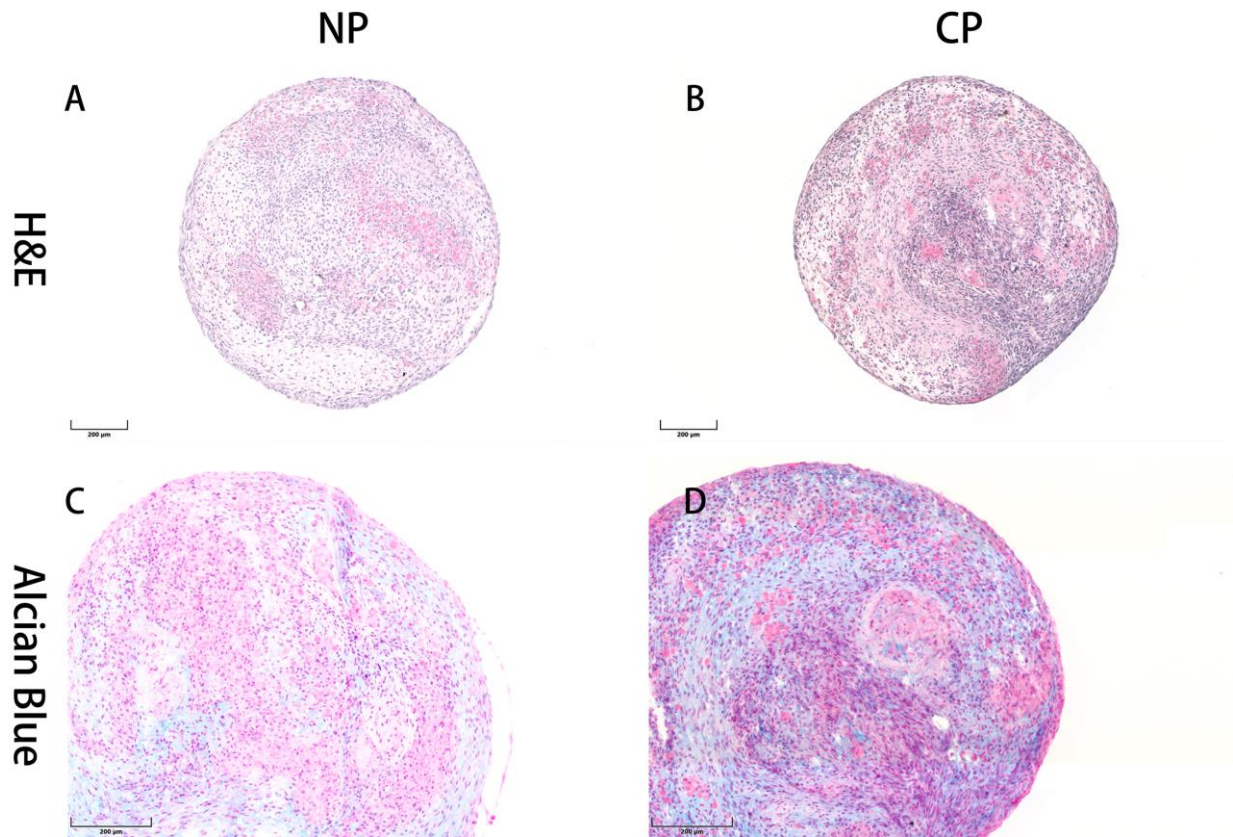


Figure 7. H&E and Alcian blue staining of day 3D hADSCs pellets cultured in either normal (A, C) and chondrogenic medium (B, D) at day 28. H&E staining of the 3D hADSCs pellet cultures in normal medium (**NP**) (A) indicate cells that appear more fibroblastic in morphology than compared to 3D hADSCs pellets in chondrogenic medium (**CP**) (B). Alcian blue staining shows extensive GAG proteoglycan formation with cellular and connective tissue formation in the **CP** group (D) compared with the **NP** 3D pellets (C), where hADSCs/differentiated chondrocytes are seen organizing themselves into specific cell and tissue layers. Magnification 20x (Bar scales: 200 μm).

5.6 Immunofluorescence analyses

Immunofluorescent staining for type II collagen and aggrecan expressions, markers for general chondrogenesis, was performed to compare matrix formation in chitosan scaffolds between chondrogenic induction and control group at day 7, 14 and 28.

Collagen type II (**Fig.8**) and ACAN (**Fig.9**) were detected in **CS** group with substantial increases in the deposition of these proteins being visualized as the culture period progressed. On the other hand, only limited fluorescent signals were observed in the **NS** group (**Fig.8, 9**). As for type I collagen, this matrix protein was minimally expressed in both **CS** and **NS** groups (**Fig.10**) with the deposition only increasing marginally by day 28 of *in vitro* culture.

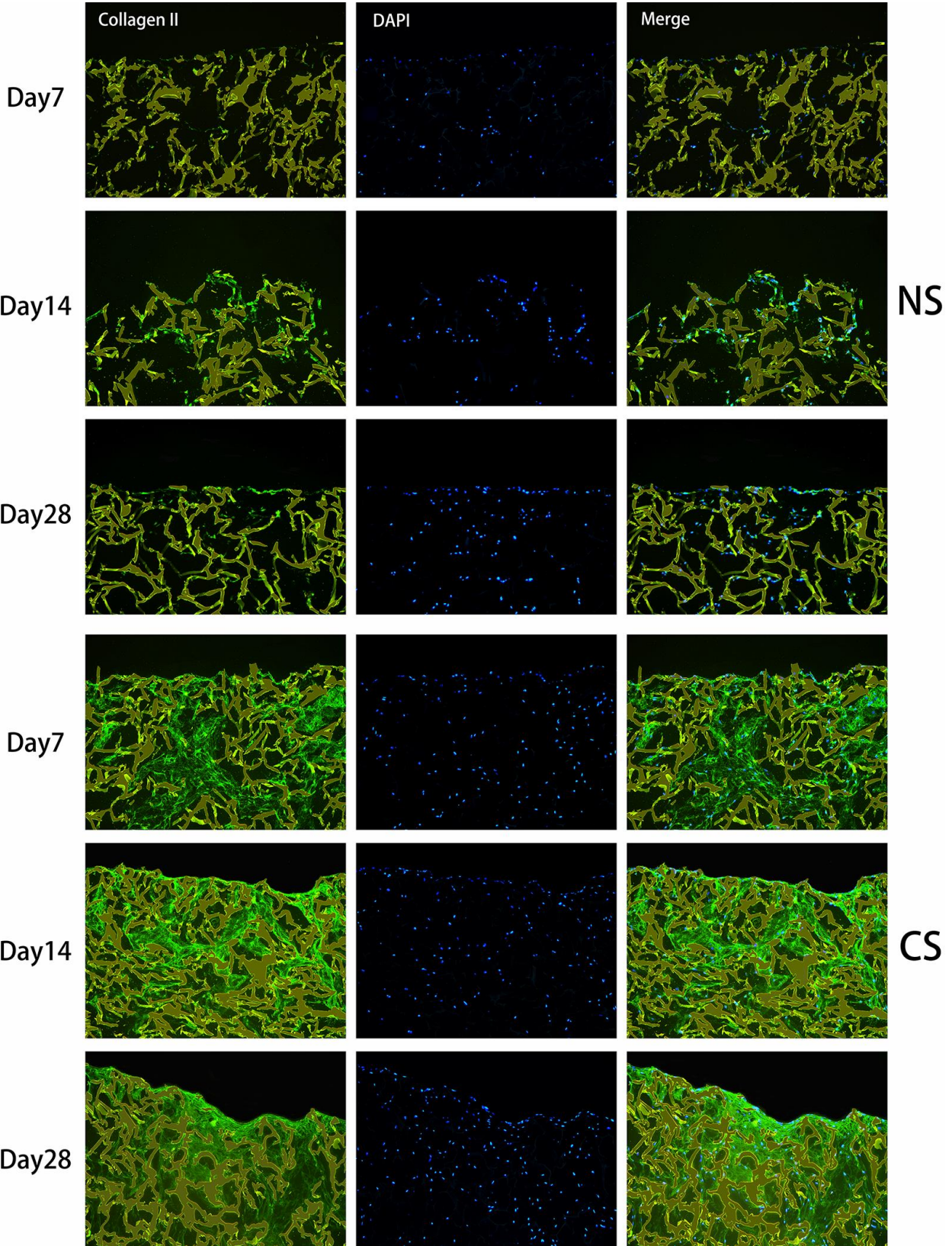


Figure 8. Immunofluorescence staining of collagen type II (**green**) at day 7, 14 and 28 in chitosan scaffolds with hADSCs cultured in normal (**NS**) or chondrogenic medium (**CS**). The chitosan scaffold fluoresced **yellow**. Cartilage matrix collagen type II protein was detected minimally in the **NS** group where cells (**blue fluorescence**), are seen lining the micropore surfaces of the chitosan scaffolds, depositing the matrix protein over the 28 day culturing period. Through the addition of the chondrogenic medium in the **CS** group, the fluorescent signal of both collagen type II and cells increased substantially and the periphery and microporous inner structures of the chitosan scaffolds are seen filling up with collagen type II matrix proteins. Magnification set a 10x.

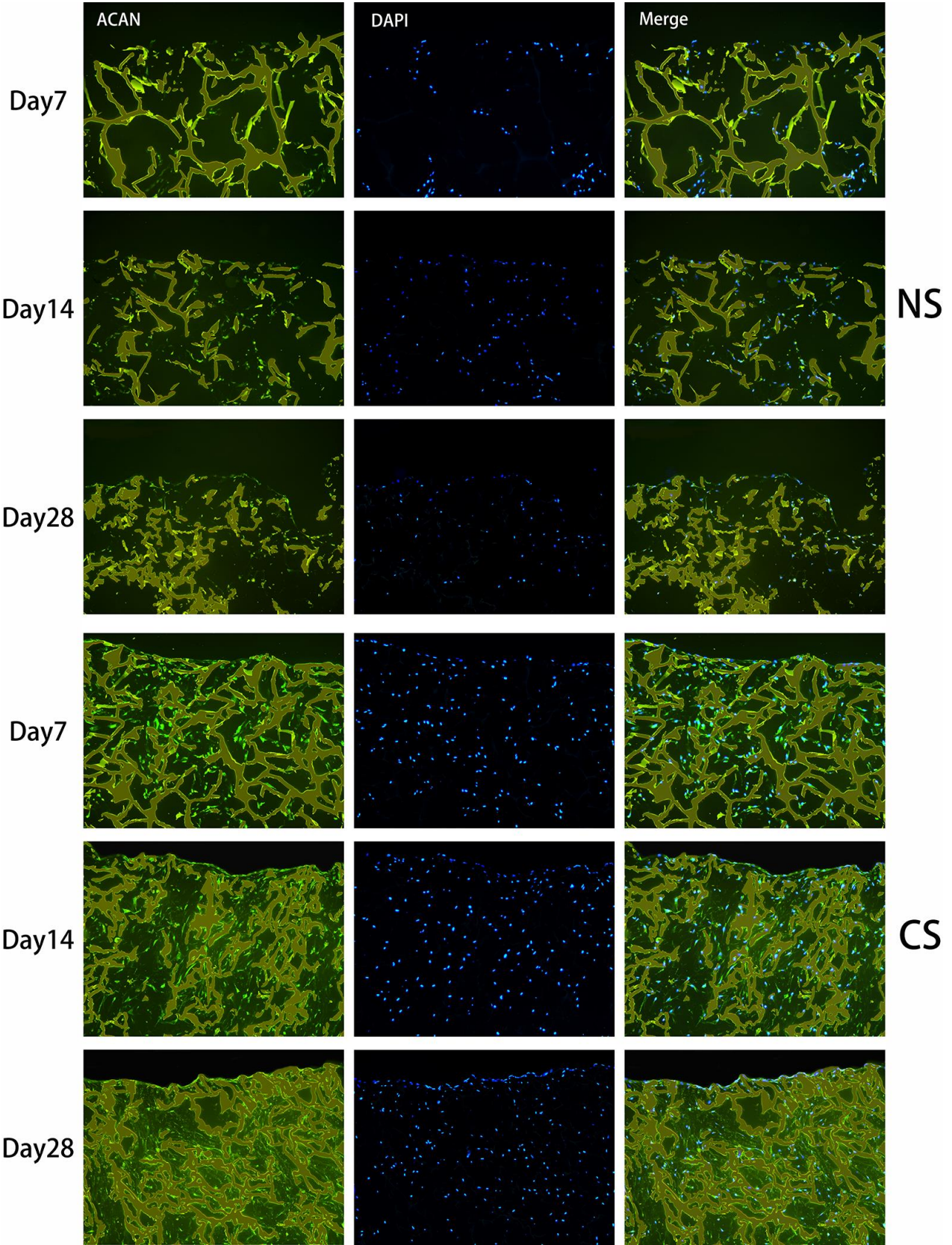


Figure 9. Immunofluorescence staining of aggrecan (**green**) at day 7, 14 and 28 in chitosan scaffolds with hADSCs cultured in normal (**NS**) or chondrogenic medium (**CS**). The chitosan scaffold fluoresced **yellow**. Aggrecan was detected minimally in the **NS** group where cells (**blue fluorescence**), are seen lining the micropore surfaces of the chitosan scaffolds, depositing the signaling protein on and within the extracellular cartilage-like matrix and on the surface topography of the chitosan devices, respectively, over the 28 day culturing period. Through the addition of the chondrogenic medium in the **CS** group, the fluorescent signal of aggrecan increased substantially both in the periphery and microporous inner structures of the chitosan scaffolds. Magnification set a 10x.

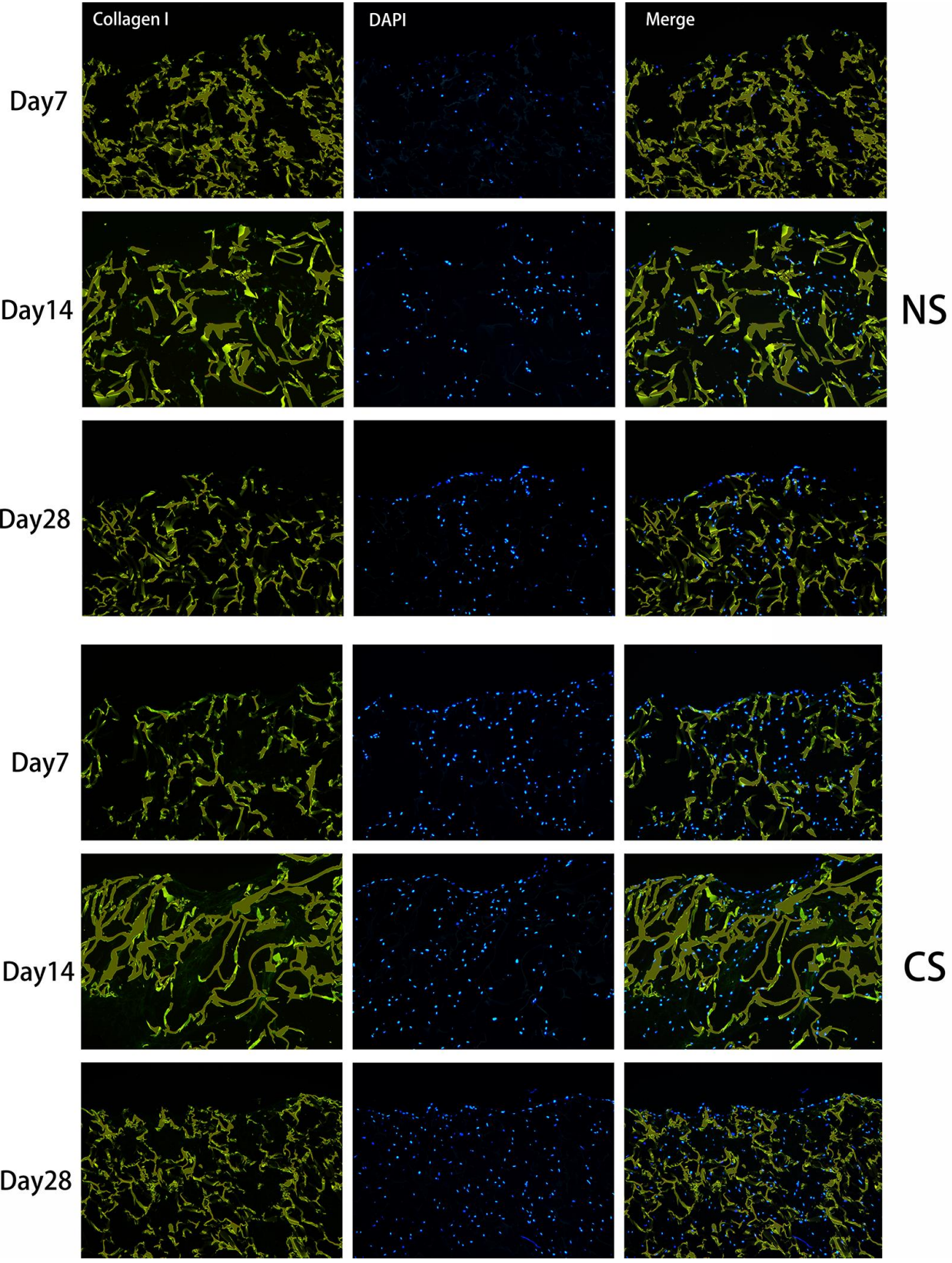


Figure 10. Immunofluorescence staining of collagen type I (**green**) at day 7, 14 and 28 in chitosan scaffolds with hADSCs cultured in normal (**NS**) or chondrogenic medium (**CS**). The chitosan scaffold fluoresced **yellow**. Osteogenic collagen type I was not detected in the **NS** group and only very minimally in **CS** group. Only the cells (**blue fluorescence**) are seen to increase in numbers especially in the chondrogenic cultured **CS** group. Magnification set a 10x.

5.7 QRT-PCR results

5.7.1 Optimum Amplification Temperature of all gene primers

In order to determine the optimum temperature at which to run all gene primer sequences at to facilitate proper gene amplification during qRT-PCR reactions a temperature gradient (55°C – 65°C) run was performed. The results (**Table 2**) showed that the optimum temperature range for most gene primer pairs was 55°C to 65°C with *Col1A1* temperature range beginning only at 58°C with *Col2A1* temperature range being 55°C - 58°C. This therefore limited the optimum annealing temperature between all gene primers to an overall annealing temperature of 58°C such that PCR reaction runs remained standardized.

Table 2. Temperature gradient range at which primers amplified relevant gene sequences

Gene Primers	Temperature Gradient Range (°C)										
	55	55.5	56.5	58	59	60.3	61.7	62.9	63.9	64.6	65
COL1A1											
COMP											
SOX9											
COL2A1											
COL10A1											
ACAN											
TBP											
GAPDH											
RNA28S											
POLR2e											
RPLP0											
SDHA											
ACTB											
RPL13a											

 Optimum Temperature Range per gene primer pair

 Optimum Temperature shared between all primers

5.7.2 Standardized cDNA quantity for optimum qRT- PCR reactions

In order to maximize the number of genes to be analyzed within the present study a standard curve analysis in the form of Cq values in **Table 3** was generated to see at which cDNA amount of differentiated hADSCs into chondrocytes (Chond.) a reasonable amplification threshold was maintained. Results revealed that the best Cq values were generated at a cDNA quantity of 40 ng with Cq values increasing as the cDNA amounts decreased to 2.5ng. However, all Cq values between all reference genes were below the 35 Cq mark and had similar numerical differences at a specific cDNA quantity with little to no overall variation in the Cq value, which meant that any cDNA quantity can be utilized with 10ng of cDNA being chosen as the best amount for all qRT-PCR reactions.

Table 3. The mean Cq of reference genes at different cDNA quantities

Reference gene	Stem cell and differentiation status	Cq at cDNA quantity				
		2.5 ng	5 ng	10 ng	20 ng	40 ng
<i>SDHA</i>	hADSCs (Chond.)	27.07	26.09	25	24	23.07
<i>POLR2e</i>	hADSCs (Chond.)	27.75	26.37	25.5	24.4	24.23
<i>TBP</i>	hADSCs (Chond.)	28.07	27.1	26.1	25.2	24.04
<i>ACTB</i>	hADSCs (Chond.)	25.45	23.96	22.7	21.8	21.19
<i>RPL13a</i>	hADSCs (Chond.)	18.26	17.03	15.9	15	13.85
<i>RNA28S4</i>	hADSCs (Chond.)	13.95	12.84	11.9	10.8	11.3
<i>GAPDH</i>	hADSCs (Chond.)	23.04	22.02	20.6	19.6	18.53
<i>RPLP0</i>	hADSCs (Chond.)	25.32	24.07	22.9	21.9	21.39

Note: Chond. = hADSCs differentiated into chondrocytes.

5.7.3 GeNorm: Stability and optimal number of reference gene(s)

Generated GeNorm reference gene expression stability results of chondrogenic differentiated hADSCs were ranked as *RPLP0*, *ACTB*, *TBP*, *POLR2e*, *RNA28S4*, *GAPDH*, *SDHA* and *RPL13a*. All of the M values of the amplified reference genes were below 0.15, demonstrating that all the reference genes chosen were stable. Among them, the *RPLP0*, *ACTB* were the most stable reference genes expressed in chondrogenic differentiated hADSCs (**Fig. 11 A**). As shown in **Figure 11**, the optimal number of reference genes to use for normalization during a qRT-PCR analysis was 3 to 4 for the chondrogenic differentiated hADSCs group as generated by GeNorm (**Fig. 11 B**), because the V3/V4 value was the lowest.

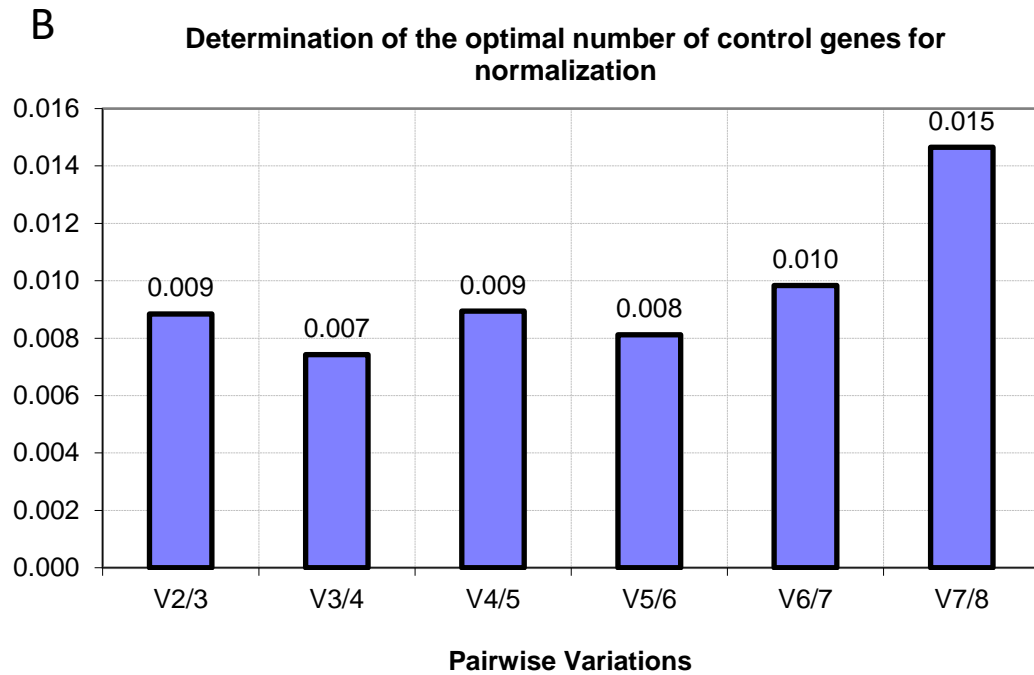
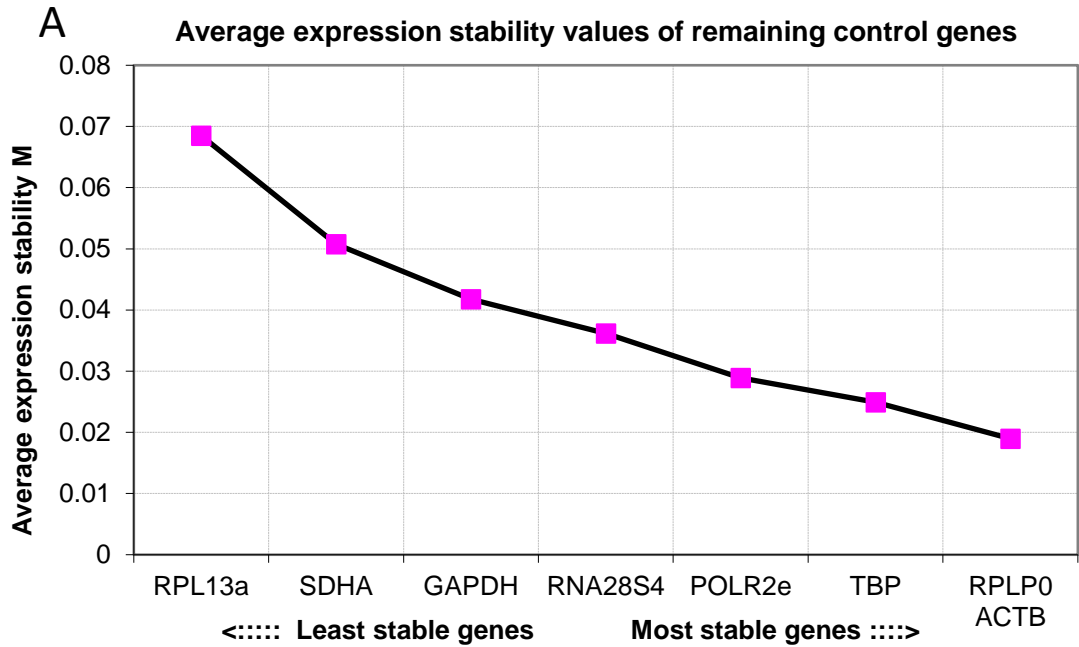


Figure 11. Ranking of reference genes by average expression stability (A) and optimal number of reference genes for normalization (B) for qRT-PCR assays, utilizing the GeNorm algorithm for chondrogenic differentiated hADSCs.

5.7.4 qRT-PCR of *in vitro* chondrogenic differentiation

To evaluate chondrogenic gene expression between the **NS**, **CS**, **NP** and **CP** groups, relative qRT-PCR gene analysis was performed on *in vitro* samples, monitoring the relative change in transcription of *ACAN*, *COL1A1*, *COL2A1*, *COL10A1*, *SOX9* and *COMP*. The results represent a snapshot of the above genes at day 7, 14 and 28 after culturing with chondrogenic induction medium or normal medium in PCSs or in the form of a 3D pellet. The results have been normalized to four control genes (*ACTB*, *RPLP0*, *TBP*, *POLR2e*), expressed as log₁₀NRQ (calibrated normalized relative quantities, CNRQ). Relative expression of every gene in different groups but at the same time point is shown in **Fig.12**, whereas of every gene at different time points but in the same group is shown in **Fig.13**.

ACAN and *COL2A1* expressions were found to be up-regulated in all the groups (**Fig.12A, C**) and increased significantly by day 28 in both pellets and cell-scaffold constructs treated with chondrogenic medium ($p < 0.05$, $p < 0.001$) (**Fig.13 A, C**). In **CS** and **CP** groups, the two genes increase in expression with *in vitro* culture time, in contrast to this in **NS** group *ACAN* and *COL2A1* decreased (**Fig.13 A, C**). Compared to **NP** and **NS** groups, *ACAN* expression in the **CP** and **CS** groups was significantly higher ($p < 0.001$) at all three-time points (**Fig.12A**). The expression of *COL2A1* at day 28 was significantly greater in the chondrogenic group compared to the control group of both pellets and cell-scaffold constructs, the difference is larger for the scaffolds (**Fig.12C**).

COMP and *SOX9* were both up-regulated in **CS** group at all time points and the expression increased significantly by day 14 but decreased at day 28 (**Fig.13E, F**). In

the **CP** group, these two genes increased significantly over time. Conversely, in the **NS** and **NP** groups, the expression of *COMP* (**Fig.13E**) was down-regulated. *SOX9* expression in **NP** was down-regulated at day 7 and 14, but up-regulated at day 28, whereas being down-regulated at all time points in **NS** group (**Fig. 12F, 13F**). Changes across the pellets and cell-scaffold constructs were significant. Compared to **NP** and **NS**, respectively, *COMP* expression was significantly higher in chondrogenic groups at all time points (**Fig.12E, F**).

COL1A1 and *COL10A1* were included as negative markers for differentiation towards articular cartilage (Benya, et al. 1978; Long and Linsenmayer 1995), as they are indicators of the endochondral bone formation. *COL1A1* was significantly up-regulated in the **CS** group at day 7 and 14 but was down-regulated at day 28. The **NS** group had a similar tendency as the **CS** group over the four-week culture period (**Fig.12B, 13B**). In the **NP** and **CP** groups, the expression of *COL1A1* was down-regulated at day 7 with the **NP** group showing a similar pattern of down-regulation as the **NS** group. However, the **CP** group *COL1A1* expression changed drastically by day 28 where the transcription was significantly up-regulated (**Fig.13B**). Compared to **CS**, the expression of *COL1A1* in **CP** group was significantly higher at day 28 ($p < 0.01$) (**Fig.12B**). This is characteristic for a more fibrous and less hyaline matrix production from cells under the influence of the proliferation medium. The expression of *COL10A1* was also analyzed, as the up-regulation of this gene during chondrogenesis is a known marker for chondrocyte hypertrophy indicating cartilage that is progressing towards an endochondral bone lineage rather than hyaline articular cartilage. The expression of *COL10A1* was down-regulated in all groups except for the **CS** group where the transcription increased

significantly after day 7 and was not significantly down-regulated at day 14 or 28 (**Fig.13D**). The gene expression of *ACAN*, *COL2A1*, *COMP* and *SOX9*, known chondrogenic markers, increased consistently over the 28 day culture period in both groups with chondrogenic medium (**CS & CP**), but decreased for the proliferative medium in scaffolds only (**NS**) (**Fig.13A, C, E, F**). Gene expression of *COMP* and *SOX9* only increased for pellet culture in proliferation medium (**NP, Fig.13E, F**). Interestingly, the expression of *COL10A1*, a classical hypertrophy marker, was significantly increased on day 28 in both groups treated hTGF- β_3 in relation to control, indicating a possible induction towards non-articular cartilage development by this factor (**Fig.12D**).

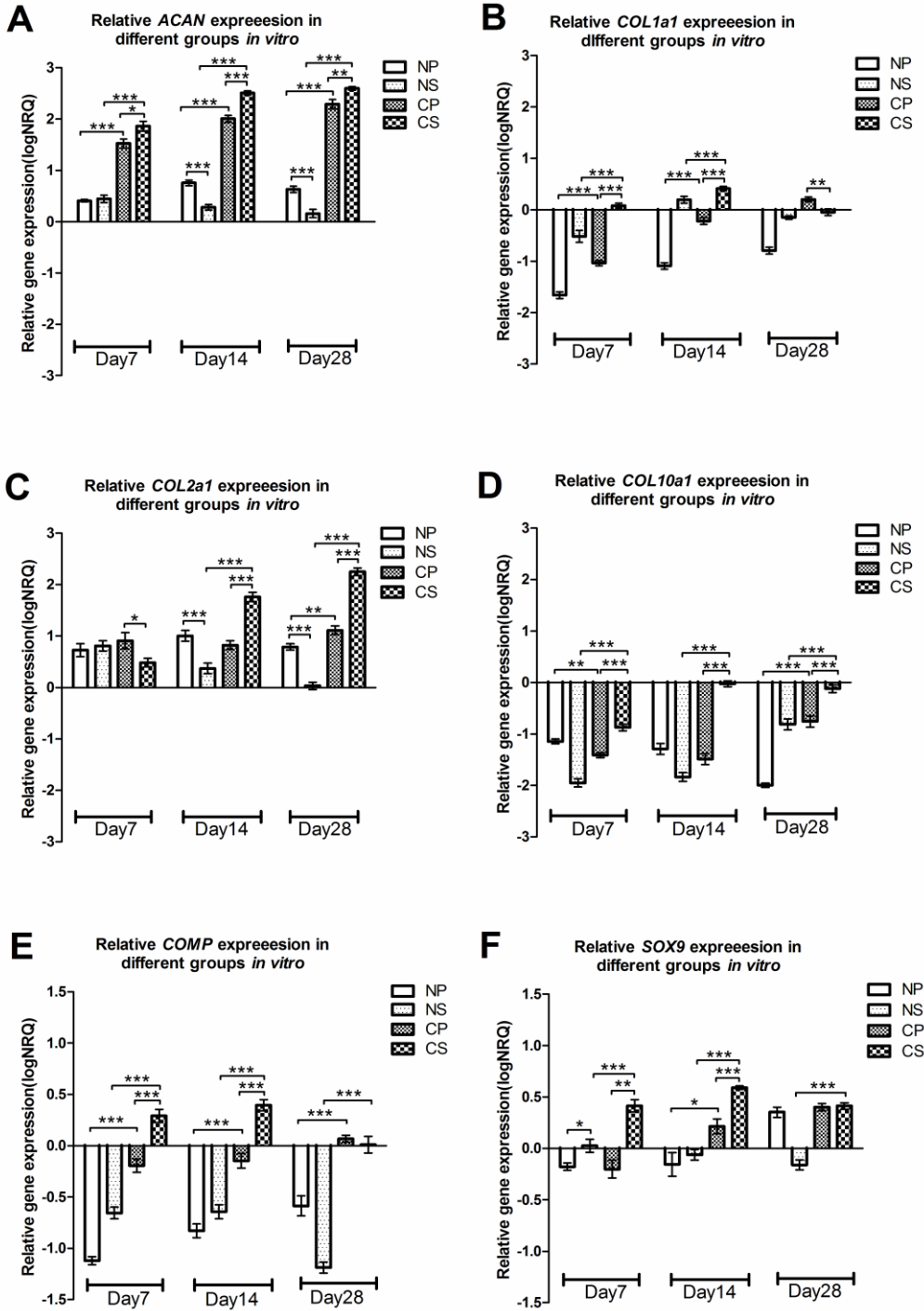


Figure 12. Relative gene expression quantity of (A) *ACAN*, (B) *COL1A1*, (C) *COL2A1*, (D) *COL10A1*, (E) *COMP* and (F) *SOX9* between all culture groups (N= normal medium; C= chondrogenic medium, P= 3D Pellet; S= chitosan scaffolds) at day 7, 14 and 28. (* $p < 0.05$, ** $p < 0.01$, *** $p < 0.001$).

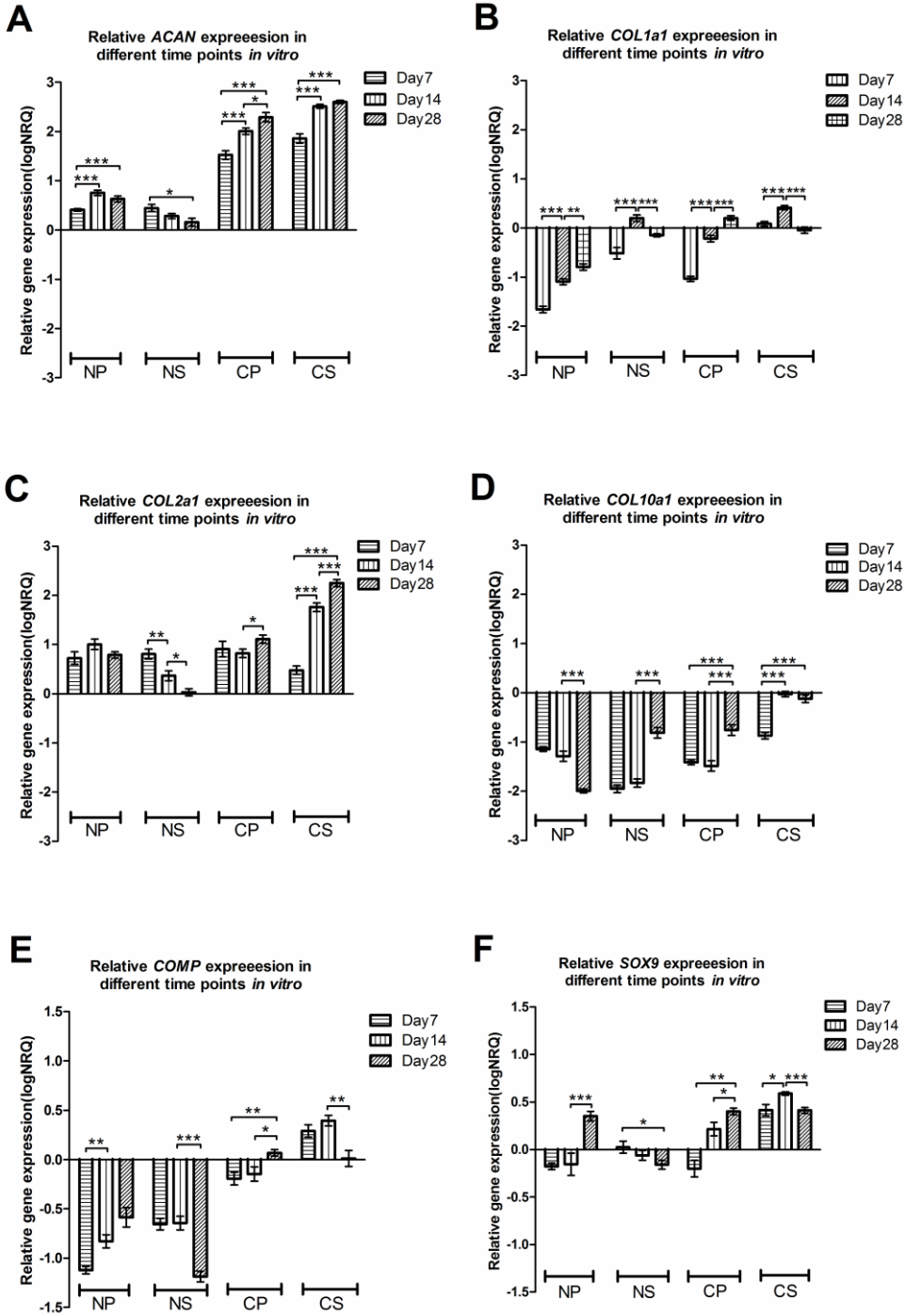


Figure 13. Relative gene expression quantity of (A) *ACAN*, (B) *COL1A1*, (C) *COL2A1*, (D) *COL10A1*, (E) *COMP* and (F) *SOX9* between all time points (day 7, 14 and 28) per 3D pellet or chitosan scaffolds culture medium group (N= normal medium; C= chondrogenic medium, P= 3D Pellet; S= chitosan scaffolds). (* $p < 0.05$, ** $p < 0.01$, *** $p < 0.001$).

6. Discussion

Articular cartilage regeneration remains a challenging clinical issue (Chiang and Jiang 2009; Veronesi, et al. 2014; Wang, et al. 2014), despite several promising approaches using adapted scaffold materials and a combination of stem cells with growth factors (Dahlin, et al. 2014a; Fan, et al. 2006; Jeong, et al. 2008; Mizuta, et al. 2004; Wakitani, et al. 1994). The biomaterials used in cartilage tissue engineering need to be highly biocompatible, biodegradable, possess the proper biomechanical properties and the appropriate geometric configurations that further support cell attachment, proliferation and differentiation (Awad, et al. 2004; Cavallo, et al. 2013; Correa and Lietman 2017). As such, the ideal scaffold would need to be one that mimics the extracellular cartilage matrix with the properties including biocompatibility, bioactivity, biomimetic, bioresponsibility and biodegradability, retaining the phenotype of differentiated stem cells in both form and function on which they can proliferate three-dimensionally (Vinatier and Guicheux 2016). One such material is chitosan, a polysaccharide derived from the exoskeleton of arthropods, which has shown to be one of the more beneficial substances that has been widely investigated and used in various derivative forms in tissue engineering and specific clinical applications (Rodriguez-Vazquez, et al. 2015). Especially scaffolds composed of poly(lactic-co-glycolic acid) (PLGA)/ chitosan devices have been shown to support chondrocyte development, Schwann cell differentiation from hADSCs and form articular cartilage in a lagomorph model over 12 weeks (Fang, et al. 2014; Razavi, et al. 2015; Zhang, et al. 2015). As for cells compared with differentiated chondrocytes isolated from cartilage and BM-MSCs isolated from bone marrow, hADSCs can be harvested in large amounts and are readily accessible (Zheng, et al. 2005). Human ADSCs are capable of maintaining the stable phenotype of

differentiated cells and can easily be differentiated into chondrocyte-like cells *in vitro* under specific culture conditions, maintaining the chondrogenic phenotype even *in vivo* after transplantation (Lo Furno, et al. 2016; Xie, et al. 2012; Zheng, et al. 2006). However, hADSCs cultured on a pure, elastic and porous scaffold composed of glutaraldehyde-crosslinked chitosan have so far not been shown to support chondrocyte development and articular cartilage matrix formation. The use of such carriers with specific morphogenic factors was therefore assessed in this study with the aim of developing improved systems for the formation of articular cartilage *in vivo*. The viability, proliferation and differentiation capacity of hADSCs cultivated in lyophilized scaffolds of glutaraldehyde-crosslinked chitosan *in vitro* increased stably with culture time over the 28 days. The scaffolds with their porous structure enabled migration, accumulation and proliferation of hADSCs. Results from the Live/Dead assay demonstrated that the hADSCs exhibited excellent adhesion and biocompatibility on the biomaterial. Comparing the results from this assay from 14 days onward between chondrogenic and control groups, a strongly enhanced cell proliferation in chitosan scaffolds with chondrogenic differentiation medium demonstrated a positive interaction of the carrier with the morphogens. Scanning electron microscopy clearly showed cells colonizing the scaffolds, forming a dense fibrous matrix with denser layers occurring on the periphery of the device by 28 days.

A subsequent marker for the chitosan's capacity to induce chondrogenesis was the detection of both glycosaminoglycans (GAGs) synthesis, a key marker for chondrogenesis, that is part of the extracellular matrix of cartilage as well as collagen type II transcription and translation together with *ACAN* and *SOX9* up-regulation. Human

ADSCs cultured on PCSs with normal medium did not show substantial formation of GAGs compared to both their corresponding 3D pellet controls or the PCSs cultured in chondrogenic medium (**Fig. 5, 7**), which was further supported by both immunofluorescent analysis and qRT-PCR assays (**Fig. 8, 9, 12, 13**). *COL2A1* was significantly down-regulated by day 28 in the **NS** group with *ACAN* and *SOX9* also decreasing substantially compared to the same normal medium group with 3D pelleted hADSCs. The relative gene expression assay of chondrogenic differentiation markers further supported this finding where whilst *ACAN* and *SOX9* expression increased in both PCSs groups irrelevant of medium type, *COL2A1* was only significantly up-regulated in the PCSs with hADSCs in chondrogenic medium (**Fig.12, 13**). The transcription factor *SOX9* is an early marker for chondrogenesis that regulates collagen type II and cartilage-specific matrix synthesis by activating the *COL2A1* and *ACAN* (Lefebvre, et al. 2001; Ng, et al. 1997). Another study previously demonstrated that *SOX9* was also expressed in proliferating and pre-hypertrophic chondrocytes, however, is down-regulated in hypertrophic chondrocytes (Suchorska, et al. 2017). From the present results, therefore, it is clear that the chitosan device on its own can induce hADSCs to undergo differentiation towards a cartilage lineage but does not possess the necessary capacity to form a cartilage matrix without the addition of a subsequent stimulant which was the case for the **CS** and **CP** groups where hTGF- β_3 was used.

In the chondrogenic differentiation process of MSCs, members of the TGF- β superfamily play a crucial role (Darling and Athanasiou 2005a; Ude, et al. 2017; Wu, et al. 2013). The combination of TGF- β and other factors was adopted in the current work to promote the chondrogenic differentiation of hADSCs, simulate the environment of an articular

implant site and also promote faster proliferation and differentiation of hADSCs towards a chondrogenic lineage (Dahlin, et al. 2014b; Lopez-Ruiz, et al. 2018). In particular, hTGF- β_3 has been shown to possess the ability to promote cartilage repair and accelerate cartilage differentiation with gene expression studies demonstrating that a correlation exists between cartilage formation and the differentiation of hADSCs (Diekman, et al. 2010; Wu, et al. 2013). A previous study documented that TGF- β_1 and TGF- β_3 was shown to have a similar effect on cell proliferation, gene expression and cartilage biosynthetic activity in ADSCs cultured in alginate beads (Estes, et al. 2006). Cals et al (Cals, et al. 2012) reported that no significant differences in total collagen and GAG formation could be observed among MSCs cultured in medium containing the three TGF- β isoforms, respectively. Some other previous studies found that TGF- β_3 was more efficient and potent than TGF- β_1 in enhancing hADSCs and MSCs chondrogenic differentiation (Barry, et al. 2001a; Liu, et al. 2010b). Other studies again have also shown that TGF- β_3 is very beneficial for cartilage as it stimulates chondrocytes *in vitro* to induce the elevation of proteoglycan and the production of collagen type II (Darling and Athanasiou 2005a; Toh, et al. 2010; Ude, et al. 2017). Therefore, in this study, we applied hTGF- β_3 (10 ng/ml) to induce chondrogenesis of hADSCs, finding similar results of induced chondrogenesis, stimulated proliferation and promotion of differentiation into chondrocytes.

Immunofluorescence staining of collagen type II and aggrecan (**Fig.8, 9**), histological staining of Alcian blue for GAG (**Fig.5,7**) confirmed that the chondrogenic treated medium groups with hTGF- β_3 , **CP** and **CS**, showed an increase both on the translational and transcriptional level of most cartilage relevant markers. Especially in the **CS** group,

histological and immunofluorescence staining demonstrated that GAG and collagen type II synthesis was significantly increased during the *in vitro* culturing for 28 days. Results of qRT-PCR, with *ACAN*, *COL2A1* and *SOX9* expression levels all increased significantly; suggest that the chitosan scaffold provides a far superior microenvironment that allows for the adhesion, proliferation and differentiation of cells under the influence of the chondrogenic medium. However, the crucial question of every cartilage culture *in vitro* is whether the matrix formed is hyaline or contains significant amounts of collagen I, and if it is hyaline cartilage, the matrix develops towards stable articular cartilage rather than progresses towards hypertrophy and mineralization.

ACAN, *COL2A1* and *SOX9* are markers that are generally utilized to monitor if any cartilage formation had occurred irrelevant of the type (Dehne, et al. 2010; Unguryte, et al. 2016; Wehrli, et al. 2003). On the other hand, *COL1A1*, *COL10A1* and *COMP* are classical markers to further differentiate what type of cartilage is being formed (Dehne, et al. 2009; Dehne, et al. 2010; Grogan, et al. 2014). Articular cartilage has superior load-bearing and mechanical properties and is free of collagen I (Sophia Fox, et al. 2009; Wilson, et al. 2006), while hyaline cartilage formed during endochondral ossification during embryogenesis for certain skeletal bones, is characterized by the early appearance of collagen X (Bahney, et al. 2014). In our study, collagen type I immunofluorescence staining was undetectable in all groups at day 7, 14 and 28, suggesting possible articular hyaline cartilage formation, but the gene expression patterns for *COL1A1* and *COL10A1* revealed that cultures were not purely articular and already programmed towards hypertrophy. Neither *COL10A1* nor *COL1A1* decreased significantly as is typically expected during articular cartilage formation but where either

inactive or slightly elevated over the 28 days of culture. In the 3D pelleted hADSCs with the chondrogenic medium, a similar gene expression pattern was observed but here *COL1A1* increased slightly at day 28 with *COL10A1* being significantly down-regulated over all time points. Taken that hADSC cultures in chitosan without chondrogenic treatment did not show elevated *COL10A1* expression, indicating that perhaps the scaffolds interacted with hTGF- β_3 absorbing the morphogen into their matrix and thereby affecting cellular functionality. Chitosan scaffolds on their own have a limited capacity to direct stem cell differentiation, as has been suggested elsewhere (Sampath and Reddi 1981; Urist, et al. 1967). On the other hand, the fact that hTGF- β_3 alone may not be a suitable morphogen for articular cartilage formation has also been demonstrated before (Klar, et al. 2014; Ripamonti, et al. 2016; Ripamonti, et al. 2008), as it seems to cause endochondral cartilage ossification rather than true articular cartilage development.

Alternatively, *COMP* a member of the thrombospondin (TSP) calcium-binding protein family, is predominantly expressed in the pericellular matrix of maturing articular cartilage chondrocytes (DiCesare, et al. 1994). Accumulating evidence suggests that *COMP* plays a crucial role in the regulation of chondrogenesis and endochondral bone formation, where it functions to stabilize the extracellular matrix of articular cartilage by maintaining the structural integrity of the cartilage by interacting with aggrecan, collagen type II, type IX and fibronectin (Chen, et al. 2007; Di Cesare, et al. 2002; Hecht, et al. 2005; Mann, et al. 2004). *COMP* demonstrates significant expression in chondrocytes, osteoblasts, tenocytes, and ligament cells but not in undifferentiated mesenchymal cells (Barry, et al. 2001b; Zaucke, et al. 2001). In our study *COMP* was down-regulated in **NP**

and **NS (Fig.13E)** groups. Conversely, *COMP* expressed in the **CS** group was significantly higher compared to the **NS** group (**Fig.12E**) at all time points but was seen to decrease significantly at the day 28 (**Fig.13E**). We therefore can also hypothesize, based on the *COMP* results that the growth of the cartilage could have progressed in two stages within the scaffolds. In the first stage, a possible cell growth phase occurred, which is characterized by significantly increased cell proliferation up to 14 days (**Fig.2B**). In the second stage, described as cell differentiation and tissue deposition phase, decreased proliferation and increased collagen type II and proteoglycan were deposited possibly due to continued stimulation by hTGF- β_3 . It is plausible then that the extracellular cartilage matrix within the first two weeks of *in vitro* culturing could have tended towards an endochondral bone cartilage lineage, which was then slowly being transforming into mature articular hyaline cartilage. As the hADSCs differentiate into chondrocytes, the cells begin to produce extracellular matrix rich in aggrecan and *COMP*. This can be confirmed by the increasing expression of *collagen type II*, *ACAN* and the rare *COL1A1* in scaffolds which is also supported by the immunofluorescence (**Fig.8, 9, 10**) and histological results (**Fig.5 D-F**). Through the possible abundance in matrix molecules, a negative feedback loop could be reducing the expression of specific genes effectively regulating chondrocyte metabolism towards an articular matrix rather than an endochondral bone structure (Hamid, et al. 2012; Mardani, et al. 2013; Tsuda, et al. 2003).

As such it is clear, that despite the results of chitosan being a viable compound that has the potential to cause articular cartilage formation, the appropriate biomaterials utilized to either simulate *in vivo* environments of cartilage *in vitro* or that are supplemented

within cartilage inducing bioreactor devices needs to be re-assessed and adjusted as the current findings clearly suggest that hTGF- β_3 is an ineffective articular cartilage inducing factor. Clearer molecular mechanisms need to be established in future experiments that ensure that viable articular cartilage repair clinically is stimulated and maintained after biomaterial implantation.

7. Conclusion

From the study, it is therefore evident, that chitosan remains a viable and highly beneficial biomaterial that even on its own and at very low percentages has good qualities to stimulate and differentiate stem cells into chondrocytes. Indeed, hADSCs have once again proven to be a competitive alternative stem cell type that has many excellent qualities to differentiate into the appropriate cell types if the correct signal, either substratum or soluble, is provided. However, from the results, with the usage of chondrogenic differentiation medium with hTGF- β_3 , the appropriate morphogen effect on cells and even tissue types through exact molecular expression patterns over time needs to be more clearly defined so as to prevent possible misinterpretation of considered candidate signaling growth factors, intended to enhance the development and re-formation of the target tissue type, without causing unwanted results. If this is correctly solved, then it can be stated that the cell-scaffold based construct may provide the basis as a viable alternative to autologous cartilage grafts that are more efficient and effective at regenerating articular cartilage defects clinically.

8. Summary

Human adipose-derived adult stem cells (hADSCs) are considered to be an alternative cell source for cell-based cartilage repair because of their ability to differentiate into a chondrogenic phenotype in response to specific environmental signals such as growth factors or biomimetic bioreactors. In this study, the chondrogenic differentiation and cartilage formation potential of hADSCs seeded onto three-dimensional (3D) porous, glutaraldehyde-crosslinked chitosan scaffolds in comparison to pellet culture *in vitro* after cultivation for up to 28 days, was investigated. By culturing either in normal or chondrogenic medium containing human transforming growth factor beta 3 (hTGF- β_3), the cartilage formation potential was assessed using a combination of viability, proliferation, scanning electron microscopy and quantitative RT-PCR assays. Scanning electron microscopy coupled with Alcian blue staining, Collagen type 2 immunofluorescence and the up-regulation of *COL2A1*, *ACAN*, *COMP* and *SOX9* in untreated and treated (chondrogenic medium) chitosan scaffolds and 3D cell pellets, indicated a progression of hADSCs towards a chondrogenic lineage that showed the capacity to form a cartilage matrix within the porous structure of the chitosan scaffolds. Whilst limited articular cartilage matrix formation was found within samples with hADSCs under non-chondrogenic *in vitro* conditions, supported by the down-regulation of both *COL1A1* and *COL10A1*, the inverse was true for those in the chondrogenic medium where hADSCs were seen depositing “a” cartilaginous matrix but that seemed to be predestined for endochondral ossification. These results clearly re-iterate the potential of hADSCs as a viable and reliable stem cell source that together with chitosan scaffolds have the potential to re-form or heal cartilaginous defect sites of an articular nature.

However, hTGF- β_3 does not appear as a suitable chondrogenic differentiation morphogen as it seems to cause endochondral ossification.

9. Zusammenfassung

Humane, von adipösem Gewebe gewonnene Erwachsene Stammzellen (hADSCs) gelten aufgrund ihrer Fähigkeit, unter spezifische Umweltsignale wie Wachstumsfaktoren oder biomimetische Bioreaktoren, sich in chondrogenischen Phänotyp zu differenzieren, als alternative Zellquelle für die zellbasierte Knorpelreparatur. In dieser Studie wurde das chondrogene Differenzierungs- und Knorpelbildungspotential von hADSCs auf dreidimensionalen (3D) porösen, Glutaraldehyd-vernetzten Chitosangerüsten im Vergleich zu Pelletkulturen *in vitro* nach Kultivierung bis zu 28 Tagen untersucht. Durch Kultivieren entweder in normalem oder chondrogenem Medium, das den humanen transformierenden Wachstumsfaktor beta 3 (hTGF- β_3) enthielt, wurde das Knorpelbildungspotential unter Verwendung einer Kombination von Viabilität, Proliferation, Rasterelektronenmikroskopie und quantitativen RT-PCR-Assays bewertet. Rasterelektronenmikroskopie gekoppelt mit Alcian-Blau-Färbung, Collagen-Typ-2-Immunfluoreszenz und die Hochregulation von *COL2A1*, *ACAN*, *COMP* und *SOX9* in unbehandelten und behandelten (Chondrogen-Medium) Chitosan-Gerüsten und 3D-Zellpellets zeigten eine Progression von hADSCs hin zu einer chondrogenischen Zellen Linie welches die Fähigkeit zeigte, eine Knorpelmatrix innerhalb der porösen Struktur der Chitosangerüste zu bilden. Während begrenzte artikulare Knorpelmatrixbildung innerhalb der Proben mit hADSCs unter nicht-chondrogenem *in vitro* Bedingungen gefunden wurde, unterstützt durch die Herunterregulierung von sowohl *COL1A1* als auch *COL10A1*, war die Umkehrung für jene in chondrogenem Medium zutreffend, wo hADSCs eine Knorpelmatrix deponierten welches mehr zur Endochondralen Ossifikation prädestiniert gewesen zu schien. Diese Ergebnisse zeigen ein deutlich das Potenzial von hADSCs als eine lebensfähige und

zuverlässige Stammzellquelle, die zusammen mit Chitosangerüsten das Potenzial haben, knorpelige Defektstellen von einer artikularen Natur neu zu bilden oder zu heilen. Humanes TGF- β_3 erscheint jedoch nicht als ein geeignetes chondrogenes Differenzierungsmorphogen zu sein, da es eine Knorpelmatrix Deponierung verursacht welches zur Endochondralen Ossifikation neigt.

10. References

Alborzi, A., et al.

1996Endochondral and intramembranous fetal bone development: osteoblastic cell proliferation, and expression of alkaline phosphatase, m-twist, and histone H4. *J Craniofac Genet Dev Biol* 16(2):94-106.

Angermann, P., K. Harager, and L. L. Tobin

2002Arthroscopic chondrectomy as a treatment of cartilage lesions. *Knee Surg Sports Traumatol Arthrosc* 10(1):6-9.

Argun, M., et al.

1993The chondrogenic potential of free autogenous periosteal and fascial grafts for biological resurfacing of major full-thickness defects in joint surfaces (an experimental investigation in the rabbit). *Tokai J Exp Clin Med* 18(3-6):107-16.

Armstrong, C. G., and D. L. Gardner

1977Thickness and distribution of human femoral head articular cartilage. Changes with age. *Ann Rheum Dis* 36(5):407-12.

Awad, H. A., et al.

2004Chondrogenic differentiation of adipose-derived adult stem cells in agarose, alginate, and gelatin scaffolds. *Biomaterials* 25(16):3211-22.

Bae, D. K., K. H. Yoon, and S. J. Song

2006Cartilage healing after microfracture in osteoarthritic knees. *Arthroscopy* 22(4):367-74.

Bahney, C. S., et al.

2014Stem cell-derived endochondral cartilage stimulates bone healing by tissue transformation. *J Bone Miner Res* 29(5):1269-82.

Bara, J. J., et al.

2014 Bone marrow-derived mesenchymal stem cells become antiangiogenic when chondrogenically or osteogenically differentiated: implications for bone and cartilage tissue engineering. *Tissue Eng Part A* 20(1-2):147-59.

Barry, F., et al.

2001a Chondrogenic differentiation of mesenchymal stem cells from bone marrow: differentiation-dependent gene expression of matrix components. *Exp Cell Res* 268(2):189 - 200.

—

2001b Chondrogenic differentiation of mesenchymal stem cells from bone marrow: differentiation-dependent gene expression of matrix components. *Exp Cell Res* 268(2):189-200.

Benya, P. D., S. R. Padilla, and M. E. Nimni

1978 Independent regulation of collagen types by chondrocytes during the loss of differentiated function in culture. *Cell* 15(4):1313-21.

Bondarava, M., et al.

2017 Osseous differentiation of human fat tissue grafts: From tissue engineering to tissue differentiation. *Sci Rep* 7:39712.

Breinan, H. A., et al.

1997 Effect of cultured autologous chondrocytes on repair of chondral defects in a canine model. *J Bone Joint Surg Am* 79(10):1439-51.

Brighton, C. T., and R. M. Hunt

1986 Histochemical localization of calcium in the fracture callus with potassium pyroantimonate. Possible role of chondrocyte mitochondrial calcium in callus calcification. *J Bone Joint Surg Am* 68(5):703-15.

Brittberg, M., et al.

1994 Treatment of deep cartilage defects in the knee with autologous chondrocyte transplantation. *N Engl J Med* 331(14):889-95.

Bruder, S. P., and A. I. Caplan

1989 Cellular and molecular events during embryonic bone development. *Connect Tissue Res* 20(1-4):65-71.

Buckwalter, J. A.

1998 Articular cartilage: injuries and potential for healing. *J Orthop Sports Phys Ther* 28(4):192-202.

Bustin, S. A., et al.

2009 The MIQE guidelines: minimum information for publication of quantitative real-time PCR experiments. *Clin Chem* 55(4):611-22.

Cals, F. L., et al.

2012 Effects of transforming growth factor-beta subtypes on in vitro cartilage production and mineralization of human bone marrow stromal-derived mesenchymal stem cells. *J Tissue Eng Regen Med* 6(1):68-76.

Campbell, C. J.

1969 The healing of cartilage defects. *Clin Orthop Relat Res* 64:45-63.

Campbell, C. J., et al.

1963 The Transplantation of Articular Cartilage. An Experimental Study in Dogs. *J Bone Joint Surg Am* 45:1579-92.

Caplan, A. I., et al.

1997 Principles of cartilage repair and regeneration. *Clin Orthop Relat Res* (342):254-69.

Cavallo, C., et al.

2013 Chondrogenic differentiation of bone marrow concentrate grown onto a hyaluronan scaffold: Rationale for its use in the treatment of cartilage lesions. *J Biomed Mater Res A* 101(6):1559-70.

Centers for Disease, Control, and Prevention

1994 Arthritis prevalence and activity limitations--United States, 1990. *MMWR Morb Mortal Wkly Rep* 43(24):433-8.

Chandy, T., and C. P. Sharma

1990 Chitosan--as a biomaterial. *Biomater Artif Cells Artif Organs* 18(1):1-24.

Chen, F. H., et al.

2007 Interaction of cartilage oligomeric matrix protein/thrombospondin 5 with aggrecan. *J Biol Chem* 282(34):24591-8.

Chen, H., et al.

2011 Characterization of subchondral bone repair for marrow-stimulated chondral defects and its relationship to articular cartilage resurfacing. *Am J Sports Med* 39(8):1731-40.

Chiang, H., and C. C. Jiang

2009 Repair of articular cartilage defects: review and perspectives. *J Formos Med Assoc* 108(2):87-101.

Chomczynski, P., and K. Mackey

1995 Short technical reports. Modification of the TRI reagent procedure for isolation of RNA from polysaccharide- and proteoglycan-rich sources. *Biotechniques* 19(6):942-5.

Correa, D., and S. A. Lietman

2017 Articular cartilage repair: Current needs, methods and research directions. *Semin Cell Dev Biol* 62:67-77.

Costa-Pinto, A. R., R. L. Reis, and N. M. Neves

2011 Scaffolds based bone tissue engineering: the role of chitosan. *Tissue Eng Part B Rev* 17(5):331-47.

Csaki, C., P. R. Schneider, and M. Shakibaei

2008 Mesenchymal stem cells as a potential pool for cartilage tissue engineering. *Ann Anat* 190(5):395-412.

Cui, L., et al.

2009 Repair of articular cartilage defect in non-weight bearing areas using adipose derived stem cells loaded polyglycolic acid mesh. *Biomaterials* 30(14):2683-93.

Curl, W. W., et al.

1997 Cartilage injuries: a review of 31,516 knee arthroscopies. *Arthroscopy* 13(4):456-60.

da Silva Meirelles, L., P. C. Chagas, and N. B. Nardi

2006 Mesenchymal stem cells reside in virtually all post-natal organs and tissues. *J Cell Sci* 119(Pt 11):2204-13.

Dahlin, R. L., et al.

2014a Articular chondrocytes and mesenchymal stem cells seeded on biodegradable scaffolds for the repair of cartilage in a rat osteochondral defect model. *Biomaterials* 35(26):7460-9.

Dahlin, R. L., et al.

2014b TGF-beta3-induced chondrogenesis in co-cultures of chondrocytes and mesenchymal stem cells on biodegradable scaffolds. *Biomaterials* 35(1):123-32.

Darling, E. M., and K. A. Athanasiou

2005a Growth factor impact on articular cartilage subpopulations. *Cell Tissue Res* 322(3):463-73.

2005b Rapid phenotypic changes in passaged articular chondrocyte subpopulations. *J Orthop Res* 23(2):425-32.

Day, T. F., and Y. Yang

2008 Wnt and hedgehog signaling pathways in bone development. *J Bone Joint Surg Am* 90 Suppl 1:19-24.

de Crombrughe, B., et al.

2000 Transcriptional mechanisms of chondrocyte differentiation. *Matrix Biol* 19(5):389-94.

de Crombrughe, B., V. Lefebvre, and K. Nakashima

2001 Regulatory mechanisms in the pathways of cartilage and bone formation. *Curr Opin Cell Biol* 13(6):721-7.

De Ugarte, D. A., et al.

2003 Comparison of multi-lineage cells from human adipose tissue and bone marrow. *Cells Tissues Organs* 174(3):101-9.

Dehne, T., et al.

2009 Chondrogenic differentiation potential of osteoarthritic chondrocytes and their possible use in matrix-associated autologous chondrocyte transplantation. *Arthritis Res Ther* 11(5):R133.

Dehne, T., et al.

2010 Gene expression profiling of primary human articular chondrocytes in high-density micromasses reveals patterns of recovery, maintenance, re- and dedifferentiation. *Gene* 462(1-2):8-17.

DeLise, A. M., L. Fischer, and R. S. Tuan

2000 Cellular interactions and signaling in cartilage development. *Osteoarthritis Cartilage* 8(5):309-34.

Deng, J., et al.

2013 A silk fibroin/chitosan scaffold in combination with bone marrow-derived mesenchymal stem cells to repair cartilage defects in the rabbit knee. *J Mater Sci Mater Med* 24(8):2037-46.

Dervin, G. F., et al.

2003 Effect of arthroscopic debridement for osteoarthritis of the knee on health-related quality of life. *J Bone Joint Surg Am* 85-A(1):10-9.

Dheda, K., et al.

2004 Validation of housekeeping genes for normalizing RNA expression in real-time PCR. *Biotechniques* 37(1):112-4, 116, 118-9.

Di Cesare, P. E., et al.

2002 Matrix-matrix interaction of cartilage oligomeric matrix protein and fibronectin. *Matrix Biol* 21(5):461-70.

Di Cesare, P., et al.

1994 Cartilage oligomeric matrix protein (COMP) is an abundant component of tendon. *FEBS Lett* 354(2):237-40.

Diekman, B. O., et al.

2010 Chondrogenesis of adult stem cells from adipose tissue and bone marrow: induction by growth factors and cartilage-derived matrix. *Tissue Eng Part A* 16(2):523-33.

Dolgin, E.

2017 The most popular genes in the human genome. *Nature* 551(7681):427-431.

Dwivedi, G., et al.

2017 Bone Marrow Progenitor Cells Isolated from Young Rabbit Trochlea Are More Numerous and Exhibit Greater Clonogenic, Chondrogenic, and Osteogenic Potential than Cells Isolated from Condyles. *Cartilage*:1947603517693044.

Edelson, R., R. T. Burks, and R. D. Bloebaum

1995 Short-term effects of knee washout for osteoarthritis. *Am J Sports Med* 23(3):345-9.

Elahi, K. C., et al.

2016 Human Mesenchymal Stromal Cells from Different Sources Diverge in Their Expression of Cell Surface Proteins and Display Distinct Differentiation Patterns. *Stem Cells Int* 2016:5646384.

Engebreetsen, L., S. Svenningsen, and P. Benum

1988 Poor results of anterior cruciate ligament repair in adolescence. *Acta Orthop Scand* 59(6):684-6.

Estes, B. T., et al.

2010 Isolation of adipose-derived stem cells and their induction to a chondrogenic phenotype. *Nat Protoc* 5(7):1294-311.

Estes, B. T., and F. Guilak

2011 Three-dimensional culture systems to induce chondrogenesis of adipose-derived stem cells. *Methods Mol Biol* 702:201-17.

Estes, B. T., A. W. Wu, and F. Guilak

2006 Potent induction of chondrocytic differentiation of human adipose-derived adult stem cells by bone morphogenetic protein 6. *Arthritis Rheum* 54(4):1222-32.

Fan, H., et al.

2006 Cartilage regeneration using mesenchymal stem cells and a PLGA-gelatin/chondroitin/hyaluronate hybrid scaffold. *Biomaterials* 27(26):4573-80.

Fan, W., et al.

2013Biomaterial scaffolds in cartilage-subchondral bone defects influencing the repair of autologous articular cartilage transplants. *J Biomater Appl* 27(8):979-89.

Fang, J., et al.

2014Poly(L-glutamic acid)/chitosan polyelectrolyte complex porous microspheres as cell microcarriers for cartilage regeneration. *Acta Biomater* 10(1):276-88.

Fortier, L. A., et al.

1998Isolation and chondrocytic differentiation of equine bone marrow-derived mesenchymal stem cells. *Am J Vet Res* 59(9):1182-7.

Fuller, J. A., and F. N. Ghadially

1972Ultrastructural observations on surgically produced partial-thickness defects in articular cartilage. *Clin Orthop Relat Res* 86:193-205.

Gao, J., J. Q. Yao, and A. I. Caplan

2007Stem cells for tissue engineering of articular cartilage. *Proc Inst Mech Eng H* 221(5):441-50.

Ghadially, F. N., et al.

1977Long-term results of superficial defects in articular cartilage: a scanning electron-microscope study. *J Pathol* 121(4):213-7.

Gibson, J. N., et al.

1992Arthroscopic lavage and debridement for osteoarthritis of the knee. *J Bone Joint Surg Br* 74(4):534-7.

Gilbert, J. E.

1998Current treatment options for the restoration of articular cartilage. *Am J Knee Surg* 11(1):42-6.

Gilbert, Scott F

2000 *Developmental Biology*. Sunderland (MA): Sinauer Associates, Inc.

Gillogly, S. D., M. Voight, and T. Blackburn

1998 Treatment of articular cartilage defects of the knee with autologous chondrocyte implantation. *J Orthop Sports Phys Ther* 28(4):241-51.

Gimble, J., and F. Guilak

2003 Adipose-derived adult stem cells: isolation, characterization, and differentiation potential. *Cytotherapy* 5(5):362-9.

Goldring, M. B., K. Tsuchimochi, and K. Ijiri

2006 The control of chondrogenesis. *J Cell Biochem* 97(1):33-44.

Gosset, M., et al.

2008 Primary culture and phenotyping of murine chondrocytes. *Nat Protoc* 3(8):1253-60.

Grande, D. A., and M. I. Pitman

1988 The use of adhesives in chondrocyte transplantation surgery. Preliminary studies. *Bull Hosp Jt Dis Orthop Inst* 48(2):140-8.

Grande, D. A., et al.

1989 The repair of experimentally produced defects in rabbit articular cartilage by autologous chondrocyte transplantation. *J Orthop Res* 7(2):208-18.

Grande, D. A., I. J. Singh, and J. Pugh

1987 Healing of experimentally produced lesions in articular cartilage following chondrocyte transplantation. *Anat Rec* 218(2):142-8.

Grande, D. A., et al.

1995 Repair of articular cartilage defects using mesenchymal stem cells. *Tissue Eng* 1(4):345-53.

Green, M. R., and J. V. Pastewka

1974 Simultaneous differential staining by a cationic carbocyanine dye of nucleic acids, proteins and conjugated proteins. I. Phosphoproteins. *J Histochem Cytochem* 22(8):767-81.

Grogan, S. P., et al.

2014 Influence of cartilage extracellular matrix molecules on cell phenotype and neocartilage formation. *Tissue Eng Part A* 20(1-2):264-74.

Guilak, F., D. L. Butler, and S. A. Goldstein

2001 Functional tissue engineering: the role of biomechanics in articular cartilage repair. *Clin Orthop Relat Res* (391 Suppl):S295-305.

Hall, B. K., and T. Miyake

1992 The membranous skeleton: the role of cell condensations in vertebrate skeletogenesis. *Anat Embryol (Berl)* 186(2):107-24.

Hamid, A. A., et al.

2012 Characterization of human adipose-derived stem cells and expression of chondrogenic genes during induction of cartilage differentiation. *Clinics (Sao Paulo)* 67(2):99-106.

Hangody, L., et al.

2001 Mosaicplasty for the treatment of articular defects of the knee and ankle. *Clin Orthop Relat Res* (391 Suppl):S328-36.

Harwin, S. F.

1999 Arthroscopic debridement for osteoarthritis of the knee: predictors of patient satisfaction. *Arthroscopy* 15(2):142-6.

Hatori, M., et al.

1995End labeling studies of fragmented DNA in the avian growth plate: evidence of apoptosis in terminally differentiated chondrocytes. *J Bone Miner Res* 10(12):1960-8.

Hattori, T., et al.

2010SOX9 is a major negative regulator of cartilage vascularization, bone marrow formation and endochondral ossification. *Development* 137(6):901-11.

Havers, C

1692*Osteologia Nova Sive Novae Quaedam Observationes de Ossibus*. Francofurti (New York, NY).

Hecht, J. T., et al.

2005COMP mutations, chondrocyte function and cartilage matrix. *Matrix Biol* 23(8):525-33.

Heng, B. C., T. Cao, and E. H. Lee

2004Directing stem cell differentiation into the chondrogenic lineage in vitro. *Stem Cells* 22(7):1152-67.

Hoekstra, A., H. Struszczyk, and O. Kivekas

1998Percutaneous microcrystalline chitosan application for sealing arterial puncture sites. *Biomaterials* 19(16):1467-71.

Hoffmann, B., et al.

2009Glutaraldehyde and oxidised dextran as crosslinker reagents for chitosan-based scaffolds for cartilage tissue engineering. *J Mater Sci Mater Med*.

Holtzer, H.

1964Control of Chondrogenesis in the Embryo. *Biophys J* 4:SUPPL239-55.

Homminga, G. N., et al.

1990Perichondral grafting for cartilage lesions of the knee. *J Bone Joint Surg Br* 72(6):1003-7.

Hsu, S. H., et al.

2011 Chondrogenesis from human placenta-derived mesenchymal stem cells in three-dimensional scaffolds for cartilage tissue engineering. *Tissue Eng Part A* 17(11-12):1549-60.

Huang, A. H., A. Stein, and R. L. Mauck

2010 Evaluation of the complex transcriptional topography of mesenchymal stem cell chondrogenesis for cartilage tissue engineering. *Tissue Eng Part A* 16(9):2699-708.

Huang, H., et al.

2014 A functional biphasic biomaterial homing mesenchymal stem cells for in vivo cartilage regeneration. *Biomaterials* 35(36):9608-19.

Hunt, S. A., L. M. Jazrawi, and O. H. Sherman

2002 Arthroscopic management of osteoarthritis of the knee. *J Am Acad Orthop Surg* 10(5):356-63.

Hunter, William

1743 On the structure and diseases of articulating cartilage. *Phil Trans Roy Soc* 42B:514–521.

Hunziker, E. B., M. Michel, and D. Studer

1997 Ultrastructure of adult human articular cartilage matrix after cryotechnical processing. *Microsc Res Tech* 37(4):271-84.

Hunziker, E. B., and L. C. Rosenberg

1996 Repair of partial-thickness defects in articular cartilage: cell recruitment from the synovial membrane. *J Bone Joint Surg Am* 78(5):721-33.

Ivkovic, A., et al.

2010 Articular cartilage repair by genetically modified bone marrow aspirate in sheep. *Gene Ther* 17(6):779-89.

Jacobs, J. E.

1965 Patellar Graft for Severely Depressed Comminuted Fractures of the Lateral Tibial Condyle. *J Bone Joint Surg Am* 47:842-7.

Jadin, K. D., et al.

2005 Depth-varying density and organization of chondrocytes in immature and mature bovine articular cartilage assessed by 3d imaging and analysis. *J Histochem Cytochem* 53(9):1109-19.

Jeong, W. K., et al.

2008 Repair of osteochondral defects with a construct of mesenchymal stem cells and a polydioxanone/poly(vinyl alcohol) scaffold. *Biotechnol Appl Biochem* 49(Pt 2):155-64.

Johnstone, B., and J. U. Yoo

1999 Autologous mesenchymal progenitor cells in articular cartilage repair. *Clin Orthop Relat Res* (367 Suppl):S156-62.

Joshy, S., et al.

2010 Accuracy of MRI scan in the diagnosis of ligamentous and chondral pathology in the ankle. *Foot Ankle Surg* 16(2):78-80.

Kim, H. K., M. E. Moran, and R. B. Salter

1991 The potential for regeneration of articular cartilage in defects created by chondral shaving and subchondral abrasion. An experimental investigation in rabbits. *J Bone Joint Surg Am* 73(9):1301-15.

Klar, R. M., et al.

2014 The induction of bone formation by the recombinant human transforming growth factor-beta3. *Biomaterials* 35(9):2773-88.

Kovacs, C. S.

2011 Bone development in the fetus and neonate: role of the calciotropic hormones. *Curr Osteoporos Rep* 9(4):274-83.

Kreuz, P. C., et al.

2006 Results after microfracture of full-thickness chondral defects in different compartments in the knee. *Osteoarthritis Cartilage* 14(11):1119-25.

Kronenberg, H. M.

2003 Developmental regulation of the growth plate. *Nature* 423(6937):332-6.

Landini, G., and G. Perryer

2009 Digital enhancement of haematoxylin- and eosin-stained histological images for red-green colour-blind observers. *J Microsc* 234(3):293-301.

Lawrence, R. C., et al.

1998 Estimates of the prevalence of arthritis and selected musculoskeletal disorders in the United States. *Arthritis Rheum* 41(5):778-99.

Lefebvre, V., R. R. Behringer, and B. de Crombrughe

2001 L-Sox5, Sox6 and Sox9 control essential steps of the chondrocyte differentiation pathway. *Osteoarthritis Cartilage* 9 Suppl A:S69-75.

Li, W. J., et al.

2005 A three-dimensional nanofibrous scaffold for cartilage tissue engineering using human mesenchymal stem cells. *Biomaterials* 26(6):599-609.

Liu, J., et al.

2010a PHBV and predifferentiated human adipose-derived stem cells for cartilage tissue engineering. *J Biomed Mater Res A* 94(2):603-10.

Liu, M., et al.

2013 Tissue engineering stratified scaffolds for articular cartilage and subchondral bone defects repair. *Orthopedics* 36(11):868-73.

Liu, S. Q., et al.

2010b Biomimetic hydrogels for chondrogenic differentiation of human mesenchymal stem cells to neocartilage. *Biomaterials* 31(28):7298-307.

Livesley, P. J., et al.

1991 Arthroscopic lavage of osteoarthritic knees. *J Bone Joint Surg Br* 73(6):922-6.

Lo Furno, D., et al.

2016 Potential Therapeutic Applications of Adipose-Derived Mesenchymal Stem Cells. *Stem Cells Dev.*

Loeser, R. F., et al.

2012 Osteoarthritis: a disease of the joint as an organ. *Arthritis Rheum* 64(6):1697-707.

Lohmander, L. S., et al.

2007 The long-term consequence of anterior cruciate ligament and meniscus injuries: osteoarthritis. *Am J Sports Med* 35(10):1756-69.

Loken, S., et al.

2008 Bone marrow mesenchymal stem cells in a hyaluronan scaffold for treatment of an osteochondral defect in a rabbit model. *Knee Surg Sports Traumatol Arthrosc* 16(10):896-903.

Long, F., and T. F. Linsenmayer

1995 Tissue-specific regulation of the type X collagen gene. Analyses by in vivo footprinting and transfection with a proximal promoter region. *J Biol Chem* 270(52):31310-4.

Lopez-Ruiz, E., et al.

2018 Impact of TGF-beta family-related growth factors on chondrogenic differentiation of adipose-derived stem cells isolated from lipoaspirates and infrapatellar fat pads of osteoarthritic patients. *Eur Cell Mater* 35:209-224.

Lu, C. H., et al.

2012 Improved chondrogenesis and engineered cartilage formation from TGF-beta3-expressing adipose-derived stem cells cultured in the rotating-shaft bioreactor. *Tissue Eng Part A* 18(19-20):2114-24.

Mackie, E. J., et al.

2008 Endochondral ossification: how cartilage is converted into bone in the developing skeleton. *Int J Biochem Cell Biol* 40(1):46-62.

Madhally, S. V., and H. W. Matthew

1999 Porous chitosan scaffolds for tissue engineering. *Biomaterials* 20(12):1133-42.

Maes, C., et al.

2010 Osteoblast precursors, but not mature osteoblasts, move into developing and fractured bones along with invading blood vessels. *Dev Cell* 19(2):329-44.

Mahmoudifar, N., and P. M. Doran

2010 Chondrogenic differentiation of human adipose-derived stem cells in polyglycolic acid mesh scaffolds under dynamic culture conditions. *Biomaterials* 31(14):3858-67.

Mandelbaum, B. R.

2016 Editorial Commentary: Focal Cartilage Defects in Young Patients Indicate Autologous Chondrocyte Implantation Sooner Rather Than Later. *Arthroscopy* 32(9):1917-8.

Mankin, H. J.

1982 The response of articular cartilage to mechanical injury. *J Bone Joint Surg Am* 64(3):460-6.

Mann, H. H., et al.

2004 Interactions between the cartilage oligomeric matrix protein and matrilins. Implications for matrix assembly and the pathogenesis of chondrodysplasias. *J Biol Chem* 279(24):25294-8.

Mardani, M., et al.

2013 Comparison between Chondrogenic Markers of Differentiated Chondrocytes from Adipose Derived Stem Cells and Articular Chondrocytes In Vitro. *Iran J Basic Med Sci* 16(6):763-73.

Matsusue, Y., T. Yamamuro, and H. Hama

1993 Arthroscopic multiple osteochondral transplantation to the chondral defect in the knee associated with anterior cruciate ligament disruption. *Arthroscopy* 9(3):318-21.

Messner, K., and W. Maletius

1996 The long-term prognosis for severe damage to weight-bearing cartilage in the knee: a 14-year clinical and radiographic follow-up in 28 young athletes. *Acta Orthop Scand* 67(2):165-8.

Micheli, L. J., et al.

2001 Autologous chondrocyte implantation of the knee: multicenter experience and minimum 3-year follow-up. *Clin J Sport Med* 11(4):223-8.

Mizuta, H., et al.

2004 Active proliferation of mesenchymal cells prior to the chondrogenic repair response in rabbit full-thickness defects of articular cartilage. *Osteoarthritis Cartilage* 12(7):586-96.

Morille, M., et al.

2016 PLGA-based microcarriers induce mesenchymal stem cell chondrogenesis and stimulate cartilage repair in osteoarthritis. *Biomaterials* 88:60-9.

Nejadnik, H., et al.

2010 Autologous bone marrow-derived mesenchymal stem cells versus autologous chondrocyte implantation: an observational cohort study. *Am J Sports Med* 38(6):1110-6.

Newman, A. P.

1998 Articular cartilage repair. *Am J Sports Med* 26(2):309-24.

Ng, L. J., et al.

1997 SOX9 binds DNA, activates transcription, and coexpresses with type II collagen during chondrogenesis in the mouse. *Dev Biol* 183(1):108-21.

Ochi, M., et al.

2001 Current concepts in tissue engineering technique for repair of cartilage defect. *Artif Organs* 25(3):172-9.

Ogilvie-Harris, D. J., and D. P. Fitzsialos

1991 Arthroscopic management of the degenerative knee. *Arthroscopy* 7(2):151-7.

Ohlendorf, C., W. W. Tomford, and H. J. Mankin

1996 Chondrocyte survival in cryopreserved osteochondral articular cartilage. *J Orthop Res* 14(3):413-6.

Ollier, L

1867 *Traité Expérimental et Clinique de la Régénération des os et de la Production Artificielle du Tissu Osseux* 2, Vol. Paris: Victor Masson.

Oryan, A., and S. Sahviah

2017 Effectiveness of chitosan scaffold in skin, bone and cartilage healing. *Int J Biol Macromol* 104(Pt A):1003-1011.

Pacifici, M., et al.

2006 Cellular and molecular mechanisms of synovial joint and articular cartilage formation. *Ann N Y Acad Sci* 1068:74-86.

Panadero, J. A., S. Lanceros-Mendez, and J. L. Ribelles

2016 Differentiation of mesenchymal stem cells for cartilage tissue engineering: Individual and synergetic effects of three-dimensional environment and mechanical loading. *Acta Biomater* 33:1-12.

Pascual-Garrido, C., et al.

2009 Recommendations and treatment outcomes for patellofemoral articular cartilage defects with autologous chondrocyte implantation: prospective evaluation at average 4-year follow-up. *Am J Sports Med* 37 Suppl 1:33S-41S.

Pugnaloni, A., et al.

1988 [Chitosan. Biochemical structural characteristics and bio-morphology]. *Boll Soc Ital Biol Sper* 64(2):101-8.

Quintana, L., N. I. zur Nieden, and C. E. Semino

2009 Morphogenetic and regulatory mechanisms during developmental chondrogenesis: new paradigms for cartilage tissue engineering. *Tissue Eng Part B Rev* 15(1):29-41.

Razavi, S., et al.

2015 Nanobiocomposite of poly(lactide-co-glycolide)/chitosan electrospun scaffold can promote proliferation and transdifferentiation of Schwann-like cells from human adipose-derived stem cells. *J Biomed Mater Res A* 103(8):2628-34.

Reddi, A. H.

2000 Initiation and promotion of endochondral bone formation by bone morphogenetic proteins: potential implications for avian tibial dyschondroplasia. *Poult Sci* 79(7):978-81.

Redler, L. H., et al.

2012 Management of articular cartilage defects of the knee. *Phys Sportsmed* 40(1):20-35.

Ripamonti, U., et al.

2016 The synergistic induction of bone formation by the osteogenic proteins of the TGF-beta supergene family. *Biomaterials* 104:279-96.

Ripamonti, U., et al.

2008 The induction of endochondral bone formation by transforming growth factor-beta(3): experimental studies in the non-human primate *Papio ursinus*. *J Cell Mol Med* 12(3):1029-48.

Rodriguez-Vazquez, M., et al.

2015 Chitosan and Its Potential Use as a Scaffold for Tissue Engineering in Regenerative Medicine. *Biomed Res Int* 2015:821279.

Rubak, J. M., M. Poussa, and V. Ritsila

1982 Chondrogenesis in repair of articular cartilage defects by free periosteal grafts in rabbits. *Acta Orthop Scand* 53(2):181-6.

Salim, A., A. J. Giaccia, and M. T. Longaker

2004 Stem cell differentiation. *Nat Biotechnol* 22(7):804-5; author reply 805-6.

Sampath, T. K., and A. H. Reddi

1981 Dissociative extraction and reconstitution of extracellular matrix components involved in local bone differentiation. *Proc Natl Acad Sci U S A* 78(12):7599-603.

Scammell, B. E., and H. I. Roach

1996 A new role for the chondrocyte in fracture repair: endochondral ossification includes direct bone formation by former chondrocytes. *J Bone Miner Res* 11(6):737-45.

Senn, N

1889 On the Healing of Aseptic Bone Cavities by Implantation of Antiseptic Decalcified Bone. *Ann Surg* 10(5):352-68.

Shannon, F. J., et al.

2001 Short-term benefit of arthroscopic washout in degenerative arthritis of the knee. *Int Orthop* 25(4):242-5.

Shapiro, F., S. Koide, and M. J. Glimcher

1993 Cell origin and differentiation in the repair of full-thickness defects of articular cartilage. *J Bone Joint Surg Am* 75(4):532-53.

Shelbourne, K. D., S. Jari, and T. Gray

2003 Outcome of untreated traumatic articular cartilage defects of the knee: a natural history study. *J Bone Joint Surg Am* 85-A Suppl 2:8-16.

Shin, H., S. Jo, and A. G. Mikos

2003 Biomimetic materials for tissue engineering. *Biomaterials* 24(24):4353-64.

Silver, F. H., and A. I. Glasgow

1995 Cartilage wound healing. An overview. *Otolaryngol Clin North Am* 28(5):847-64.

Sophia Fox, A. J., A. Bedi, and S. A. Rodeo

2009 The basic science of articular cartilage: structure, composition, and function. *Sports Health* 1(6):461-8.

Sprague, N. F., 3rd

1981 Arthroscopic debridement for degenerative knee joint disease. *Clin Orthop Relat Res* (160):118-23.

Stokes, D. G., et al.

2002 Assessment of the gene expression profile of differentiated and dedifferentiated human fetal chondrocytes by microarray analysis. *Arthritis Rheum* 46(2):404-19.

Stosich, M. S., and J. J. Mao

2007 Adipose tissue engineering from human adult stem cells: clinical implications in plastic and reconstructive surgery. *Plast Reconstr Surg* 119(1):71-83; discussion 84-5.

Suchorska, W. M., et al.

2017 Gene expression profile in human induced pluripotent stem cells: Chondrogenic differentiation in vitro, part A. *Mol Med Rep* 15(5):2387-2401.

Tandogan, R. N., et al.

2004 Analysis of meniscal and chondral lesions accompanying anterior cruciate ligament tears: relationship with age, time from injury, and level of sport. *Knee Surg Sports Traumatol Arthrosc* 12(4):262-70.

Tare, R. S., et al.

2005 Tissue engineering strategies for cartilage generation--micromass and three dimensional cultures using human chondrocytes and a continuous cell line. *Biochem Biophys Res Commun* 333(2):609-21.

Thompson, T. J., P. D. Owens, and D. J. Wilson

1989 Intramembranous osteogenesis and angiogenesis in the chick embryo. *J Anat* 166:55-65.

Toh, W. S., et al.

2010 Cartilage repair using hyaluronan hydrogel-encapsulated human embryonic stem cell-derived chondrogenic cells. *Biomaterials* 31(27):6968-80.

Tsuda, M., et al.

2003 Transcriptional co-activators CREB-binding protein and p300 regulate chondrocyte-specific gene expression via association with Sox9. *J Biol Chem* 278(29):27224-9.

Ude, C. C., et al.

2017The evaluation of cartilage differentiations using transforming growth factor beta3 alone and with combination of bone morphogenetic protein-6 on adult stem cells. *Cell Tissue Bank* 18(3):355-367.

Unguryte, A., et al.

2016Human articular chondrocytes with higher aldehyde dehydrogenase activity have stronger expression of COL2A1 and SOX9. *Osteoarthritis Cartilage* 24(5):873-82.

Urist, M. R., et al.

1967The bone induction principle. *Clin Orthop Relat Res* 53:243-83.

VanGuilder, H. D., K. E. Vrana, and W. M. Freeman

2008Twenty-five years of quantitative PCR for gene expression analysis. *Biotechniques* 44(5):619-26.

Veronesi, F., et al.

2014Adipose-derived mesenchymal stem cells for cartilage tissue engineering: state-of-the-art in in vivo studies. *J Biomed Mater Res A* 102(7):2448-66.

Vinatier, C., and J. Guicheux

2016Cartilage tissue engineering: From biomaterials and stem cells to osteoarthritis treatments. *Ann Phys Rehabil Med* 59(3):139-44.

Viste, A., et al.

2012Autologous chondrocyte implantation for traumatic full-thickness cartilage defects of the knee in 14 patients: 6-year functional outcomes. *Orthop Traumatol Surg Res* 98(7):737-43.

Vogel, V., and M. Sheetz

2006Local force and geometry sensing regulate cell functions. *Nat Rev Mol Cell Biol* 7(4):265-75.

Wakitani, S., et al.

1994 Mesenchymal cell-based repair of large, full-thickness defects of articular cartilage. *J Bone Joint Surg Am* 76(4):579-92.

Wang, Y., et al.

2006 Factors affecting progression of knee cartilage defects in normal subjects over 2 years. *Rheumatology (Oxford)* 45(1):79-84.

Wang, Z. J., et al.

2014 Repair of articular cartilage defects by tissue-engineered cartilage constructed with adipose-derived stem cells and acellular cartilaginous matrix in rabbits. *Genet Mol Res* 13(2):4599-606.

Warrington, J. A., et al.

2000 Comparison of human adult and fetal expression and identification of 535 housekeeping/maintenance genes. *Physiol Genomics* 2(3):143-7.

Wehrli, B. M., et al.

2003 Sox9, a master regulator of chondrogenesis, distinguishes mesenchymal chondrosarcoma from other small blue round cell tumors. *Hum Pathol* 34(3):263-9.

Wei, X., et al.

2013 Mesenchymal stem cells: a new trend for cell therapy. *Acta Pharmacol Sin* 34(6):747-54.

Widuchowski, W., J. Widuchowski, and T. Trzaska

2007 Articular cartilage defects: study of 25,124 knee arthroscopies. *Knee* 14(3):177-82.

Wilson, W., et al.

2006 Prediction of collagen orientation in articular cartilage by a collagen remodeling algorithm. *Osteoarthritis Cartilage* 14(11):1196-202.

Winter, A., et al.

2003Cartilage-like gene expression in differentiated human stem cell spheroids: a comparison of bone marrow-derived and adipose tissue-derived stromal cells. *Arthritis Rheum* 48(2):418-29.

Wu, L., et al.

2013Regeneration of articular cartilage by adipose tissue derived mesenchymal stem cells: perspectives from stem cell biology and molecular medicine. *J Cell Physiol* 228(5):938-44.

Xie, X., et al.

2012Comparative evaluation of MSCs from bone marrow and adipose tissue seeded in PRP-derived scaffold for cartilage regeneration. *Biomaterials* 33(29):7008-18.

Yamashita, F., et al.

1985The transplantation of an autogeneic osteochondral fragment for osteochondritis dissecans of the knee. *Clin Orthop Relat Res* (201):43-50.

Yang, Q., et al.

2008A cartilage ECM-derived 3-D porous acellular matrix scaffold for in vivo cartilage tissue engineering with PKH26-labeled chondrogenic bone marrow-derived mesenchymal stem cells. *Biomaterials* 29(15):2378-87.

Yasuda, K.

1997[Knee pain in the aged--pathomechanism, diagnosis, and treatment of osteoarthritis of the knee]. *Hokkaido Igaku Zasshi* 72(4):369-76.

Ye, C., et al.

2009PHB/PHBHHx scaffolds and human adipose-derived stem cells for cartilage tissue engineering. *Biomaterials* 30(26):4401-6.

Younes, I., and M. Rinaudo

2015 Chitin and chitosan preparation from marine sources. Structure, properties and applications. *Mar Drugs* 13(3):1133-74.

Zaucke, F., et al.

2001 Cartilage oligomeric matrix protein (COMP) and collagen IX are sensitive markers for the differentiation state of articular primary chondrocytes. *Biochem J* 358(Pt 1):17-24.

Zhang, K., et al.

2015 In-situ birth of MSCs multicellular spheroids in poly(L-glutamic acid)/chitosan scaffold for hyaline-like cartilage regeneration. *Biomaterials* 71:24-34.

Zhang, K., et al.

2013 Repair of an articular cartilage defect using adipose-derived stem cells loaded on a polyelectrolyte complex scaffold based on poly(L-glutamic acid) and chitosan. *Acta Biomater* 9(7):7276-88.

Zhang, L., et al.

2010 Chondrogenic differentiation of human mesenchymal stem cells: a comparison between micromass and pellet culture systems. *Biotechnol Lett* 32(9):1339-46.

Zheng, B., et al.

2006 Mouse adipose-derived stem cells undergo multilineage differentiation in vitro but primarily osteogenic and chondrogenic differentiation in vivo. *Tissue Eng* 12(7):1891-901.

Zheng, Z., et al.

2005 Effects of crystallization of polyhydroxyalkanoate blend on surface physicochemical properties and interactions with rabbit articular cartilage chondrocytes. *Biomaterials* 26(17):3537-48.

Zhou, G., et al.

2006 Repair of porcine articular osteochondral defects in non-weightbearing areas with autologous bone marrow stromal cells. *Tissue Eng* 12(11):3209-21.

11. List of figures and tables

Figure 1: The gross view of spongy-like PCS and Scanning electron microscopy images of 1% PCS at different time points in culture.....	37
Figure 2: WST-1 and PicoGreen measurements of ASCs/PCS constructs.....	39
Figure 3: Fluorescent microscopy images for the live/dead cell in scaffolds.....	41
Figure 4: H&E staining for density and distribution of cells in scaffolds.....	42
Figure 5: Alcian blue staining for GAG of cell-scaffolds.....	43
Figure 6: Macroscopic image of pellet cultures in control and chondrogenic media.....	44
Figure 7: H&E and Alcian blue staining of 4 weeks' pellet	45
Figure 8: Immunofluorescence staining of collagen II in NS and CS groups.....	48
Figure 9: Immunofluorescence staining of ACAN in NS and CS groups.....	50
Figure 10: Immunofluorescence staining of collagen I in NS and CS groups.....	52
Figure 11: Ranking of reference genes by average expression stability and optimal number of reference genes for normalization.....	55
Figure 12: Relative expression of genes in different groups.....	59
Figure 13: Relative expression of genes at different time points.....	60
Table 1: Gene primers used for optimization.....	35
Table 2: Temperature gradient range at which primers amplified relevant gene sequences ...	53
Table 3: The mean Cq of reference genes at different cDNA quantities	54

12. Abbreviations

3D	Three Dimensional
2D	Two Dimensional
ACI	Autologous Chondrocyte Implantation
MSCs	Mesenchymal Stem Cells
BM-MSCs	Bone Marrow Mesenchymal Stem Cells
ASCs	Adipose-Derived Stem Cells
ECM	Extracellular Matrix
PCS	Porous Chitosan Scaffold
GAG	Glycosaminoglycan
CHI	Chitosan
WST-1	Water-Soluble Tetrazolium-1
TGF- β	Transforming growth factor- β
BMP-6	Bone Morphogenetic Protein 6
PGA	Polyglycolic Acid
GAG	Glycosaminoglycan
QRT-PCR	Quantitative Real-Time Polymerase Chain Reaction
HTCR	Human Tissue and Cell Research
BMI	Body Mass Index
RT	Room Temperature
DMEM	Dulbecco's Modified Eagle's Medium
EDTA	Ethylenediaminetetraacetic acid
FCS	Fetal Calf Serum
ITS	Insulin Transferrin Selenium

SEM	Scanning Electron Microscope
PBS	Phosphate Buffered Saline
qRT-PCR	Quantitative real-time PCR
<i>ACAN</i>	Aggrecan
<i>COL2A1</i>	Collagen type II
<i>COL10A1</i>	Collagen type X
<i>COL1A1</i>	Collagen type I
<i>SOX9</i>	SRY (sex determining region Y)-box 9
<i>COMP</i>	Cartilage Oligomeric Matrix Protein
<i>TBP</i>	TATA-binding Protein
<i>GAPDH</i>	Glyceraldehyde 3-phosphate Dehydrogenase
<i>RNA28S4</i>	RNA 28S ribosomal 4
<i>POLR2e</i>	RNA Polymerase II Subunit e
<i>RPLP0</i>	Ribosomal Protein Lateral stalk subunit P0
<i>SDHA</i>	Succinate Dehydrogenase complex flavoprotein subunit A
<i>ACTB</i>	Actin Beta
<i>RPL13a</i>	Ribosomal Protein L13a
NP	Normal medium Pellet
CP	Chondrogenic medium Pellet
NS	Normal medium Scaffold
CS	Chondrogenic medium Scaffold
HA	Hyaluronic acid
TSP	Thrombospondin

13. Acknowledgment

I would like to thank the Director Prof. Dr. med. Dipl.-Ing. Volkmar Jansson, of the Department of Orthopedic Surgery, Physical Medicine and Rehabilitation at the University Hospital of the Ludwigs-Maximillian University of Munich in Germany for having accepted me to do my Dr. Hum. Bio. Degree in his department under the kind supervision of the Vice-Director Prof. Dr. med. Peter E. Müller.

I would like to express my deepest and sincerest gratitude eternally to the Laboratory Manager and Research Division Head of Regenerative Medicine, Dr. PhD. MSc. BSc(Hon). BSc. Roland M. Klar, of the Laboratory of Biomechanics and Experimental Orthopedics who co-supervised me in all endeavors pertaining to my project and who was a constant inspiration in my time in the Laboratory, helping me to become a better professional medical scientist. Thank you for your patience with me and the excellent support in making the project a full success.

Subsequently, I would also like to thank Dr. rer. nat. Maryna Bondarava, for originally providing me with the project idea and concept together with the adipose stem cells that she most kindly extracted for me without which the project would not have been possible to do. In this regards, as such, I would also like to thank Mr. Daniel Seitz from the Friedrich Baur Biomed Center in Bayreuth, Germany who tirelessly manufactured the high quality and numerous chitosan devices that enabled me to progress with the project.

I would also like to thank the Chinese Scholarship Council LMU Grant Initiative for having considered me as a viable candidate and provided me with the grant to permit my stay in Munich, Germany such that I could do my Dr. Hum. Bio. degree in Professor Jansson Department.

From the Laboratory a special thank you also goes out to Ms. Bärbel Schmitt, the Medical Technician in the Regenerative Medicine Division that tirelessly trained me in the various methodologies for the project.

Subsequently, I also want to say thank you to the all the other staff members in the Laboratory of Biomechanics and Experimental Orthopedics, especially Dr. techn. MScA. BEng. BSc. Yan Chevalier (Division Head of Biomechanics), Dr. rer. biol. hum. Dipl.-Ing. (FH) Matthias Woiczinski and Dipl.-Ing. (FH) Michael Kraxenberger for their kindness and warmth, in making me feel at all time welcome and part of the laboratory family.

However, my greatest love and appreciation I wish to convey to my family for their continuous support and encouragement at all times in my study and daily life including being there in both the good and bad days of the project.

最后，我用中文再次表达感谢我的父母和家人，我永远爱你们。感恩及感激在我生命中出现并在我的学习和成长道路上帮助过我的所有老师，朋友。再次深深的感谢Roland教授在课题的执行和论文的书写指导方面给予我极大的帮助。